DISCLAIMER

This report was prepared as an account of work sponsored by an agency of the United States Government. Neither the United States Government nor any agency thereof, nor any of their employees, makes any warranty, express or implied, or assumes any legal liability or responsibility for the accuracy, completeness, or usefulness of any information, apparatus, product, or process disclosed, or represents that its use would not infringe privately owned rights. Reference herein to any specific commercial product, process, or service by trade name, trademark, manufacturer, or otherwise does not necessarily constitute or imply its endorsement, recommendation, or favoring by the United States Government or any agency thereof. The views and opinions of authors expressed herein do not necessarily state or reflect those of the United States Government or any agency thereof. Reference herein to any social initiative (including but not limited to Diversity, Equity, and Inclusion (DEI); Community Benefits Plans (CBP); Justice 40; etc.) is made by the Author independent of any current requirement by the United States Government and does not constitute or imply endorsement, recommendation, or support by the United States Government or any agency thereof.

Savannah River National Laboratory®

A U.S. DEPARTMENT OF ENERGY NATIONAL LAB • SAVANNAH RIVER SITE • AIKEN, SC • USA

Probabilistic Hazard Assessment for Tornadoes, Straight-Line Wind, and Extreme Precipitation at the Savannah River Site

D. Werth

October, 2025

SRNL-STI-2024-00497

DISCLAIMER

Printed in the United States of America

Prepared for
U.S. Department of Energy

SRNL-STI-2024-00497
Revision 0

Keywords: Tornadoes, Extreme Gusts and Precipitation

Retention: *Permanent*

Probabilistic Hazard Assessment for Tornadoes, Straight-Line Wind, and Extreme Precipitation at the Savannah River Site

D. W. Werth

October, 2025

Savannah River National Laboratory is operated by Battelle Savannah River Alliance for the U.S. Department of Energy under Contract No. 89303321CEM000080

Reviews and Approvals

AUTHORS:

_____

D. W. Werth, Atmospheric Technologies Group Date

TECHNICAL REVIEWERS:

_____

B. Viner, Atmospheric Technologies Group Date

APPROVAL:

_____

S. Chiswell, Atmospheric Technologies Group Date

Executive Summary

Recent data sets for three meteorological phenomena with the potential to inflict damage on SRS facilities – tornadoes, straight-line winds, and heavy precipitation – are analyzed using appropriate statistical techniques to estimate the occurrence probabilities for these events in the future. Summaries of the results for DOE-mandated return periods and comparisons to similar calculations performed in 2013 by Werth et al. (W2013) are given.

Using tornado statistics for i) the combined states of Georgia and South Carolina, and ii) a 2º square area surrounding SRS, we calculated the probability per year of any location at SRS being struck by a tornado (the 'strike' probability) and the probability that any point will experience winds above set thresholds. The strike probability was calculated to be 7.04E-4 (1 chance in 1420) per year and tornadic wind speeds for DOE mandated return periods of 50,000 years (corresponding to wind design category 3 (WDC-3), and 125,000 years (meeting WDC-4) (USDOE, 2016) were estimated to be 132 mph and 147 mph, respectively.

By contrast, default tornado wind speeds taken from ANSI/ANS-2.3-2011 are somewhat higher: 161 mph for return periods of 50,000 years and 173 mph every 125,000 years (ANS, 2011). Although the ANS and the SRS evaluation used the same basic model (Ramsdell and Rishel, 2007), the region defined in ANS 2.3 that encompasses the SRS also includes areas of the Great Plains and lower Midwest, regions with much higher occurrence frequencies of strong tornadoes.

The SRS straight-line wind values associated with various return periods were calculated by fitting existing wind data to a GEV1 distribution and extrapolating the values for any return period from the tail of that function. For the DOE mandated return periods, we expect straight-line winds of 117 mph every 2500 years (the required WDC-3 standard) and 125 mph every 6250 years (WDC-4) at any point within the SRS. These values are similar to those from the ANS-2.3-2011 report, which has wind speeds of 125mph and 133 mph for return periods of 2500 years and 6250 years, respectively.

For extreme precipitation, we compared the fits of two different theoretical extreme-value distributions and applied the one that fit the data best for each of several accumulation periods. The DOE mandated 6-hr accumulated rainfall for return periods of 10,000 years (corresponding to precipitation design category 3 (PDC-3) and 25,000 years (PDC-4) were estimated as 9.1 inches and 10.1 inches, respectively. For the 24-hr rainfall return periods of 10,000 years and 25,000 years, total rainfall estimates were 12.02 inches and 13.17 inches, respectively, higher than comparable values provided in the W2013 report.

Table of Contents

List of Tables

List of Figures

LIST OF SYMBOLS

F/EF	Fujita/Enhanced Fujita rating
a(F,i)	Area of the i^{th} tornado of magnitude F
A(F)	Total area covered by tornadoes of rating F
FR(EF,F)	The fraction of the area of an F scale tornado that is reallocated as EF wind speed
P_{strike}	Strike probability
A_T	Total area covered by tornadoes
A_R	Total area of domain
N_{year}	Number of years of tornado record
N_F	Number of tornadoes of rating F
Awind(F)	Total area covered by wind speeds of rating F
u(F)	log mean of the area covered by tornadoes of rating F (dimensionless)
v(F)	log variance of the area covered by tornadoes of rating F (dimensionless)
E(F)	expectation value of area covered by tornadoes of magnitude F (km^2)
X_{ij}	Annual maximum wind gust/rainfall at station j in year i
$\bar{X}_j$	Multi-year average of X_{ij} at station j
s_j	Multi-year standard deviation of X_{ij} at station j
τ_{ij}	Standardized value of annual maximum wind gust/rainfall at station j in year i

k	Number of stations
n_T	Total number of observations of all the stations
n_j	Number of years of data at station j
κ	Shape parameter
α	Scale parameter
ξ	Location parameter
p	nonexceedance probability
RP_{τ_p}	Return period
τ_P	Value of τ corresponding to return period P.
CV	Coefficient of variation
X_{pj}	Annual maximum wind gust/precipitation associated with return period p at station j

List of Abbreviations

ANS	American Nuclear Society
ATG	Atmospheric Technologies Group
CDF	cumulative distribution function
CLM	Central Climatology Site
DOE	Department of Energy
EF	Enhanced Fujita Scale
F	Fujita Scale
NCDC	National Climatic Data Center
NWS	National Weather Service
PHA	Probabilistic Hazard Assessment
PNNL	Pacific Northwest National Laboratory
PWM	probability weighted moments
SPC	Storm Prediction Center
SRNL	Savannah River National Laboratory
SRS	Savannah River Site

1.0 Introduction

The Savannah River National Laboratory (SRNL) Atmospheric Technologies Group (ATG) has performed an update to the Probabilistic Hazard Assessment (PHA) for severe weather phenomena at the Savannah River Site (SRS), in accordance with Department of Energy Standard DOE-STD-1020-2016 (USDOE, 2016). The PHA is to estimate future risk from three natural hazards – tornadoes, extreme straight-line winds, and extreme precipitation. In each case, the general theory is the same – the probabilities for the future are to be calculated from the statistics of the past. This is relatively simple for events that happen often (e.g., a daily rainfall greater than of 0.25”), but it is also necessary to calculate the probabilities of events that are rare, or even that have yet to happen, which is more challenging. To accomplish this, ATG collected existing datasets of the three phenomena to quantify the probabilities of extreme events, which are uncommon and therefore difficult to quantify based on their observed frequencies of occurrence. This involved the application of existing statistical techniques to newer datasets.

Such a report was produced previously by Werth et al. (2013, henceforth W2013) and Weber et al., (1998, henceforth W98), and the same statistical methods are applied to newer, larger datasets. Our results will be compared to those of W2013 and significant differences discussed.

2.0 Site Characterization

2.1 General Climate

The following SRS climate summary is taken from Scott (2013) and WSRC (2004). The Savannah River Site region has a humid subtropical climate characterized by relatively short, mild winters and long, warm, humid summers. Summer-like conditions typically last from May through September, when the area is frequently under the influence of a western extension in the semi-permanent Atlantic subtropical anticyclone (i.e. the 'Bermuda' high). Winds in summer are light and cold fronts generally remain well north of the area. Scattered afternoon and evening thunderstorms are common, and the remnants of tropical storms and hurricanes affect the area every few years. The influence of the Bermuda high begins to diminish during the fall, resulting in lower humidity and more moderate temperatures. Average rainfall during the fall is usually the least of the four seasons.

In winter, mid-latitude low pressure systems and associated fronts often migrate through the region. As a result, conditions frequently alternate between warm, moist, subtropical air from the Gulf of Mexico region and cool, dry polar air. The Appalachian Mountains to the north and northwest of the SRS help to moderate the extremely cold temperatures associated with occasional outbreaks of Arctic air into the U.S. Consequently, fewer than one-third of winter days have minimum temperatures below freezing on average, and days with temperatures below 20°F are infrequent. Observed temperature extremes at SRS range from a record maximum of 108º F (June, 2012) to a record minimum of -3° F (January, 1985).

Tornadoes occur more frequently in spring than the other seasons of the year. Although winter and spring weather is somewhat windy (of all recorded values of sustained wind speed at 2m above the ground over 5m/s, 68% occur during January through April) temperatures are usually mild and humidity is relatively low.

Several tornadoes have occurred at or close to SRS since operations began in the 1950s, and we can evaluate their impact according to two standard tornado rating scales – i) the older Fujita-scale (F1 through F5) or ii) the newer 'enhanced' Fujita-scale (EF1 through EF5), which replaced the F-scale in early 2007. Each recorded tornado is assigned an F (before 2007) or EF rating according to an evaluation of the damage, and we can use that system to describe how severely tornadoes have affected the area near SRS.

An F2 tornado that occurred during October 1989 knocked down several thousand trees over a 16-mile path across the southern and eastern portions of the site - wind speeds were estimated by the National Weather Service (NWS) to be as high as 150 mph. Four F2 tornadoes struck forested areas of SRS on three separate days during March 1991, and considerable damage to trees was observed in the affected areas. An additional four confirmed tornadoes during that time were classified as F1 and produced relatively minor damage.

Five EF3 rated tornadoes hit the CSRA in South Carolina on April 13th, 2020, with two of these storms forming within the eastern and northern portions of SRS. At SRS, one tornado destroyed a cinder block store, snapped large swaths of trees, and caused extensive damage to homes along the path.

Because the SRS is approximately 100 miles inland, winds associated with tropical weather systems usually diminish below hurricane force before arriving on site. However, a brief wind gust associated with Hurricane Gracie, which passed to the north of SRS on September 29, 1959, was measured as high as 75 mph on an anemometer located in F-Area. On September 22, 1989, the center of Hurricane Hugo passed about 100 miles northeast of SRS. The maximum 15-minute average wind speed observed onsite during this hurricane was 46 mph. The highest observed instantaneous gust ever at SRS was 89.9 mph associated with Hurricane Helene in September of 2024. The data were collected from the onsite tower network (measurements taken at 200 feet above ground). Extreme rainfall and tornadoes, which frequently accompany tropical weather systems, usually have the most significant hurricane-related impact on SRS operations.

The average annual total precipitation at SRS is 48.40 inches. The range of annual rainfall over the period from 1952-2024 was from 28.82 inches (1954) to 73.06 inches (1964). A total of 19.6 inches was recorded at SRS in October, 1990. Of this total, 10.2 inches fell in a 48 hr period during the passage of two tropical storms. Heavy rainfalls over short durations are typically associated with slow moving thunderstorms, and rainfall amounts greater than 4 inches in 15 minutes have been observed on several occasions.

Snow of 1” or greater occurs every 3 years on average, and ice on exposed surfaces occurs an average of once every 2 years. The greatest single snowfall recorded in the SRS area (Augusta, NWS) over the period 1949-2006 was in February 1973 when 15.0 inches fell in a 24-hour period. Significant snowfalls typically melt within a day or two; consequently, heavy rain coincident with a persistent large snowpack is not expected to occur in this region.

2.2 Onsite Meteorological Data Collection

The meteorological monitoring program at SRS is conducted in a manner fully consistent with the requirements of DOE Order 458.1, Radiation Protection of the Public and the Environment (USDOE, 2011), ANSI/ANS-3.11-2024 (ANS, 2024) and DOE-HDBK-1216-2015 (USDOE, 2015). This program is documented in the SRS Meteorological Monitoring Program (Weinbeck et al., 2020). The onsite data are collected from a network of nine primary monitoring stations. Towers located at each of eight operations areas (A, C, D, F, H, K, L, and P areas) are equipped to measure wind direction, wind speed, temperature, and dew point at a height of 61 meters (m) above ground. These towers are each located within a forest canopy adjacent to the operations area to gather data representative of the prevailing surface that characterizes the Site, which is dominated by forest.

A ninth tower near N-Area, known as the Central Climatology site (CLM), is instrumented with wind, temperature, and dew point sensors at four levels: 2m (4m for wind), 18m, 36m, and 61m. The CLM site is also equipped with an automated tipping bucket rain gauge, a barometric pressure sensor, and a solar radiometer near the tower at ground level. Unlike the other towers, this tower is located in a flat, cleared area. Data from CLM are available since the early 1990s.

Data acquisition units at each station record a measurement from each instrument at 1-second intervals (newer instrumentation currently on the tower records at 0.1 second intervals). Every 15 minutes, the 1-second data are processed to generate statistical summaries for each variable, including averages and instantaneous maxima, and the results are uploaded to a relational database for permanent archival.

Additional precipitation measurements are collected from a network of 12 plastic wedge rain gauges across the SRS. These gauges are read manually by security or operations personnel once per day, usually around 6 a.m. The daily data are reported each morning, reviewed to correct obvious flaws, and manually entered into a permanent electronic database.

3.0 Probabilistic Hazard Assessment for Tornadoes

3.1 Tornado Data

Unlike many weather variables such as temperature, which can be recorded automatically, tornadoes are recorded through direct observation, and this often produces idiosyncrasies in tornado records. Different databases from equally credible sources may contradict one another, earlier records may show signs of being less accurate than later records within the same database, or tornado magnitudes may be simply misjudged. A key complexity is determining whether damage is caused by tornadoes or straight-line winds which can be difficult to discern. The latter is especially true, since tornado wind speeds are seldom measured directly and are instead estimated based on the damage inflicted on trees, buildings, etc. As we will see, these problems require adjustment to the data.

An important consideration is the domain over which the statistics are to be calculated. Datasets list tornadoes over the entire United States, but we wish to characterize the risk for the area near SRS. A domain too large (for example, encompassing parts of Oklahoma and Texas) will include data from areas that are unrepresentative of the tornado risk at SRS in South Carolina, and too small a domain will likely also produce unrepresentative results, with high magnitude tornadoes absent from the data. We will look at two domains: the combined two-state area of Georgia and South Carolina, and a 2° x 2° box centered

at SRS (approximately 225 km in length per side). A map of tornado touchdown points (Figure 3.1) reveals how northern and western Georgia tend to experience more tornadoes, with an area of generally lower frequency stretching from east central Georgia into western South Carolina. The map also reveals that no F5 or EF5 tornadoes have been recorded in Georgia or South Carolina (Fig. 3.1c), though a few have hit in eastern Alabama (not shown).

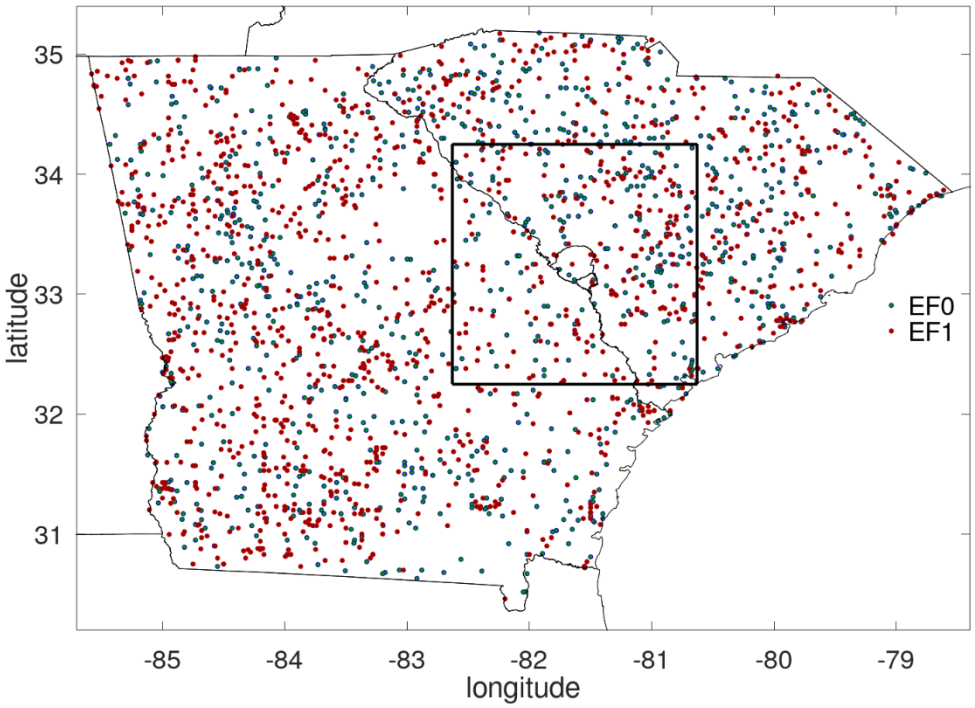

Figure 3.1 a) Map of tornado occurrences in Georgia and South Carolina for F/EF0, and F/EF1 for the period 1950-2022. The black box indicates the 2º x 2º domain centered at the SRS.

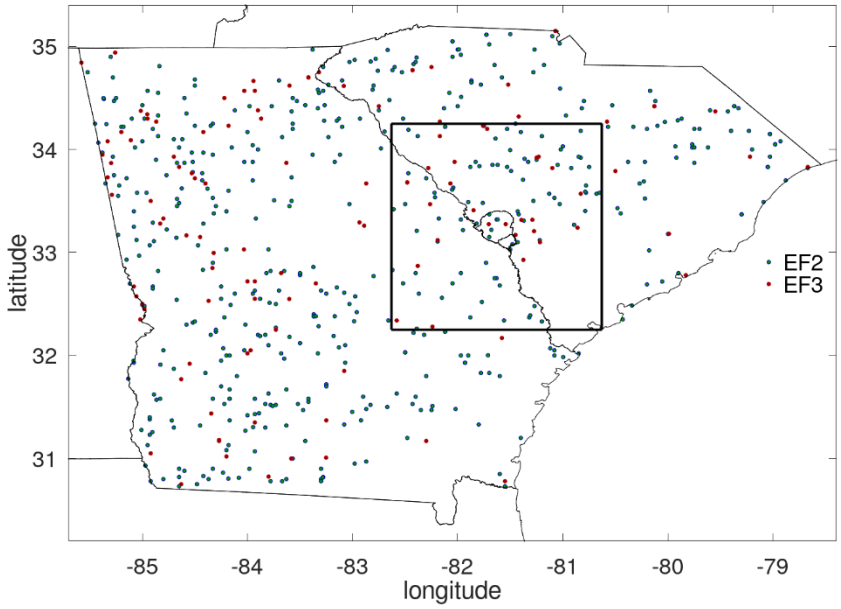

Figure 3.1 b) Map of tornado occurrences in Georgia and South Carolina for F/EF2 and F/EF3 for the period 1950-2022. The black box indicates the 2º x 2º domain centered at the SRS

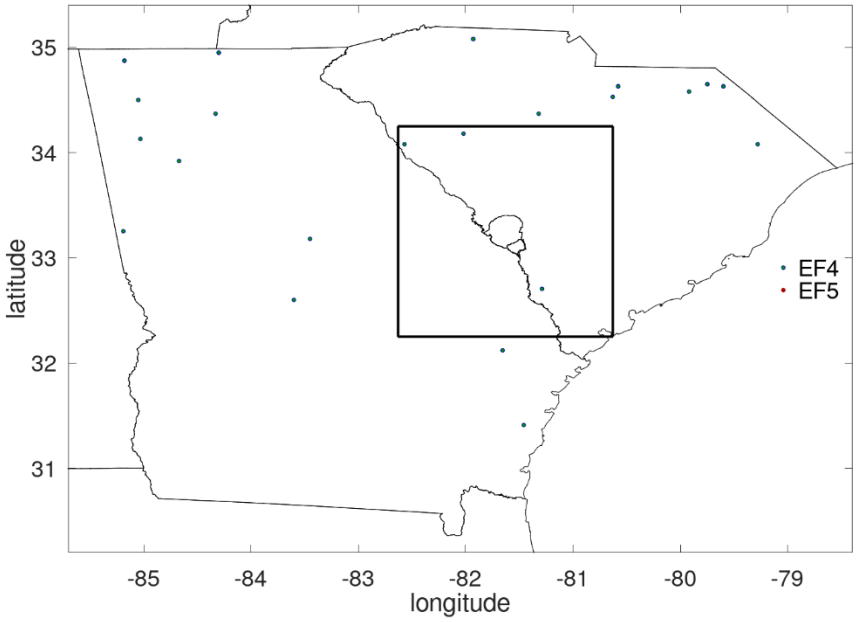

Figure 3.1 c) Map of tornado occurrences in Georgia and South Carolina for F/EF4, and F/EF5 for the period 1950-2022. The black box indicates the 2º x 2º domain centered at the SRS.

Another consideration is the scale used to classify tornado intensity – in 2007, the Fujita scale (F-scale) was replaced with the Enhanced Fujita-scale (EF-scale), which was judged to be more accurate for assigning wind speed based on the observed damage. These scales assign different wind speeds to their respective 0-5 categories; for example, an F2 represents winds from 113mph to 157mph lasting at least 3s, while an EF2 has winds from 111mph to 135mph. When calculating the numbers or cumulative damage areas of the different types, we must take care to maintain separate groupings for the F-rated and EF-rated tornadoes (though ultimately combine their results).

Several relatively complete datasets exist, and we looked at two – the Storm Prediction Center (SPC) tornado database, and a storm database maintained by the National Centers for Environmental Information (NCEI) – to compare and select one for analysis. Both datasets contain information on the date, magnitude, length and width of all recorded tornadoes, all required by DOE-STD-1020-2016, Section 4.2.3.2. A line-by-line comparison of the two datasets reveals much similarity, but also several instances in which a tornado in the SPC dataset is reported as two separate tornadoes in the NCDC dataset (Table 3.1). A time series of the number of reported F-scale tornadoes (before 2007) and EF-scale tornadoes (starting in 2007) over the two-state area per year (Fig. 3.2) are very similar, but a count reveals fewer reported tornadoes in the SPC database of all F/EF classes (Table 3.2). This by itself would not affect the results (so long as the recorded magnitude is the same), since the total tornado area is the statistic we will use to estimate tornado strike probabilities, and this is the same whether the same area is subdivided into a large number of small areas or a smaller number of larger areas. The total area affected by each magnitude, given as

$$A(F)=\sum_{i=1}^{N_F} a(F,i) \quad (1)$$

where *a(F,i)* is the area of the i^{th} tornado of magnitude F in square kilometers (for data after 2007, F in Eq. 1 is replaced by EF), and N_F is the total number of F tornadoes, tends to show larger values for the SPC data (Fig. 3.3), which will ultimately yield a greater strike probability. For consistency with W2013 (which used the SPC data), we elected to use the SPC data.

Table 3.1 Selection of January tornado (for illustration) data for NCEI (top) and SPC (bottom).

year	month	day	Length (mi)	Width (yds)
1952	1	22	1.9	350
1952	1	22	6.8	350
year	month	day	Length (mi)	Width (yds)
1952	1	22	8.7	350

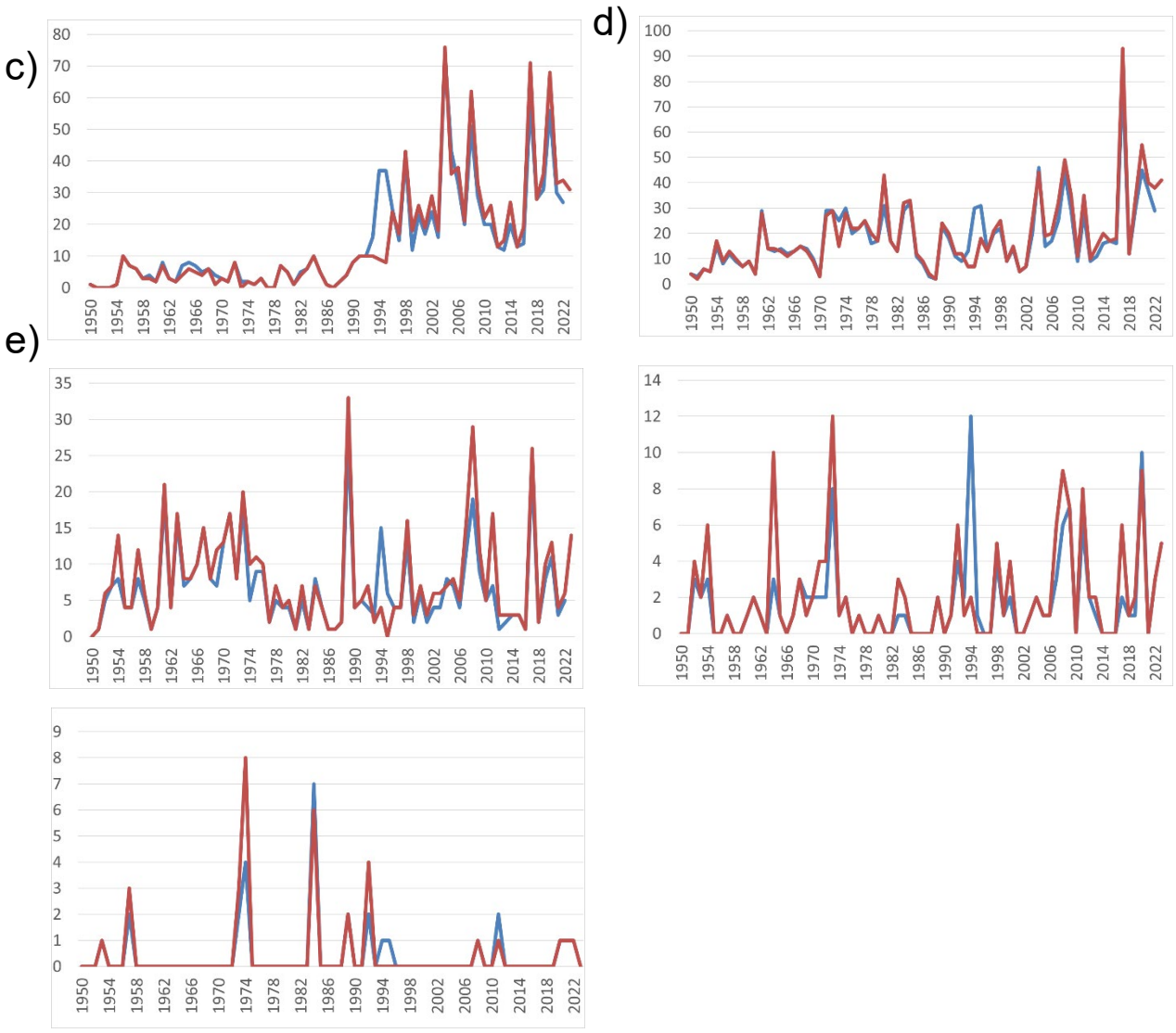

Figure 3.2 Number of tornadoes from 1950-2022 in the two-state (Georgia and South Carolina) domain for the SPC (blue) and NCEI (red) per year for the a) F0, b) F1, c)F2, d) F3, and e) F4 before 2007, after which the respective number of EF tornadoes is shown. No F5 or EF5 tornadoes occurred in either record.

Table 3.2 Number of tornadoes (between 1950-2023) of each magnitude recorded over Georgia and South Carolina in the SPC dataset.

	SPC	NCEI
F0/EF0	1035	1086
F1/EF1	1338	1447
F2/EF2	494	584
F3/EF3	120	152
F4/EF4	28	32

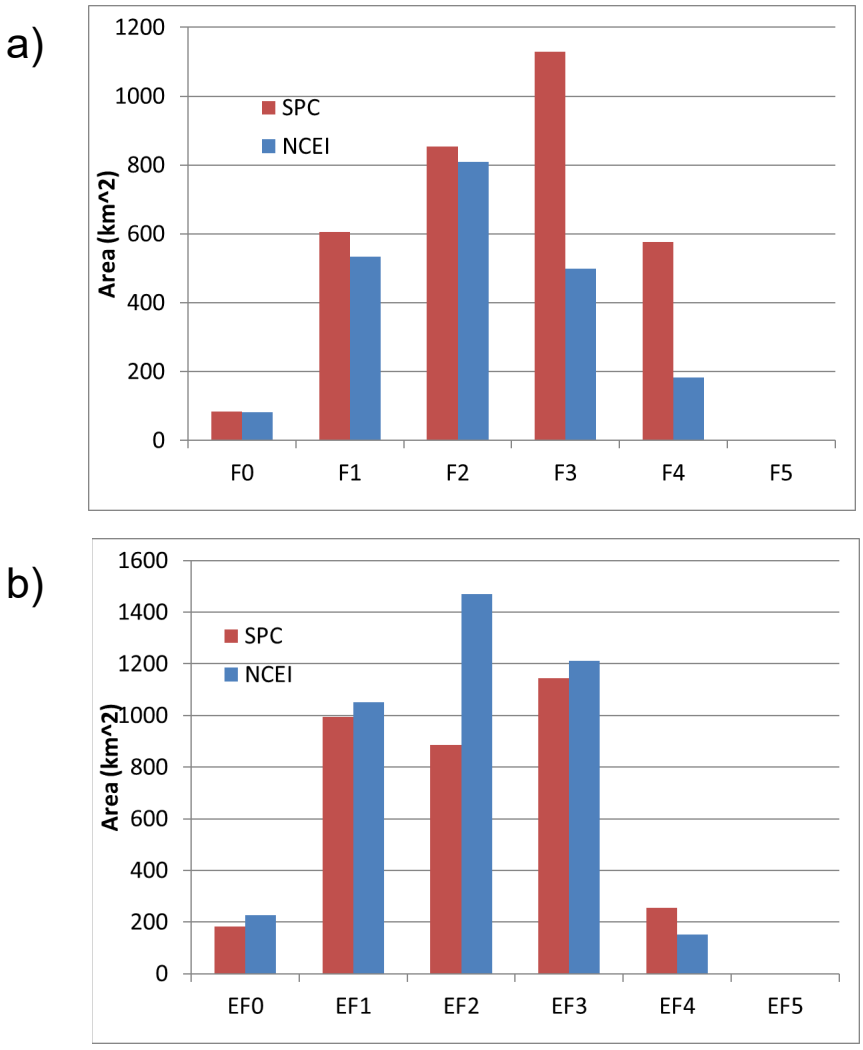

Figure 3.3 Total area covered by each a) F and b) EF category for the NCEI and SPC databases within the two-state area (Georgia and South Carolina).

3.2 Tornado Risk Model

a. Probability

An algorithm for calculating the future probability of experiencing tornadic winds above a set threshold was outlined by Ramsdell and Rishel (2007, henceforth R07) in their report on the PHA for the Pacific Northwest National Laboratory (PNNL). DOE criteria and guidance contained in 2016 (DOE-STD-1020-2016) specify in Section 4.3.2.2 that the sites utilize section 3.4 of the American Nuclear Society (ANS) ANS-2.3-2011 for the criteria and guidance on developing their site PHA, and that standard lists R07 (their reference 12) as one of two acceptable sources for an algorithm to estimate probabilities of tornadic winds. The R07 model was used in the W2013 report, and we will use it again here for consistency. The PNNL algorithm uses the actual statistics directly and does not require any special software. Therefore, most of the description below is based on the PNNL model.

Tornado risk assessments start with two premises – the probability per year of any location within a larger domain being struck by a tornado (P_{strike}) is related to the area within the domain that has been struck in the past (R07; Boissonnade et al., 2000; W98; McDonald, 1983), and the probability of any tornado having winds above certain thresholds is related to the distribution of tornado magnitudes that have occurred (R07, W98). For the first, R07 writes this simply as:

$$P_{strike} = \frac{A_T}{N_{year} A_R} \quad (2)$$

in which N_{year} is the number of years of the record, A_R is the total area of the domain of interest, and

$$A_T = \sum_{F=0}^{5} A(F) + \sum_{EF=0}^{5} A(EF) \quad (3)$$

is the total area struck by all tornadoes during the period of record. Given that the area affected by each tornado in the SPC database is provided, we can calculate P_{strike}.

For the second premise, R07 states that the probability of a point within a tornado path experiencing winds above a certain threshold is not uniform, but is proportional to the area within each tornado path above that threshold (Fig. 3.4). Tornadoes are classified according to the peak intensity, and a tornado will often evolve through several F/EF wind speed values between touchdown and dissipation. Therefore, a tornado path will comprise areas that experienced different wind speeds, with only a small fraction of the total area actually seeing the highest speeds (Fig. 3.4). Starting with the work of Reinhold and Ellingwood (1982), who calculated the fractions of an F-scale reported tornado area that experienced various F-scale wind speeds, R07 calculates a table (Table 3.1 of R07, reproduced here as Table 3.3) that is used to calculate what fraction FR(EF,F) of each F-reported area A(F) is covered by winds of each EF magnitude (A_{wind}(EF)):

$$A_{wind}(EF) = \sum_{F=0}^{5} A(F) FR(EF, F) \quad (4)$$

Our ultimate goal is to calculate the probabilities of exceeding the EF categories, so this will help convert the range of wind values from the older F rating to the current EF thresholds. For example, an F2 tornado area is partitioned as having about 62% of its total area within the EF0 wind speed range, 27% within the EF1 range, and 12% in the EF2 range (Fig. 3.4, Table 3.3), while an F0 tornado is entirely within the EF0 range

(Table 3.3). Conversely, the total area under EF0 conditions is calculated as F0+.772 F1+…0.538F5 Assuming uniform strike probability (calculated using Eq. 2) within the selected domain, and the probability that each strike will yield winds of various magnitudes calculated with FR(EF,F), we can calculate the probability per year of any point experiencing tornadic winds above a threshold as a product of the two.

Table 3.3 Tornado Area Intensity Distribution for the Point Structure Design Wind Speed Estimates (from R07).

Recorded Tornado F scale

Intensity EF Scale

	F0	F1	F2	F3	F4	F5
EF0	1	0.772	0.616	0.529	0.543	0.538
EF1		0.228	0.268	0.271	0.238	0.223
EF2			0.115	0.133	0.131	0.119
EF3				0.067	0.056	0.07
EF4					0.032	0.033
EF5						.017

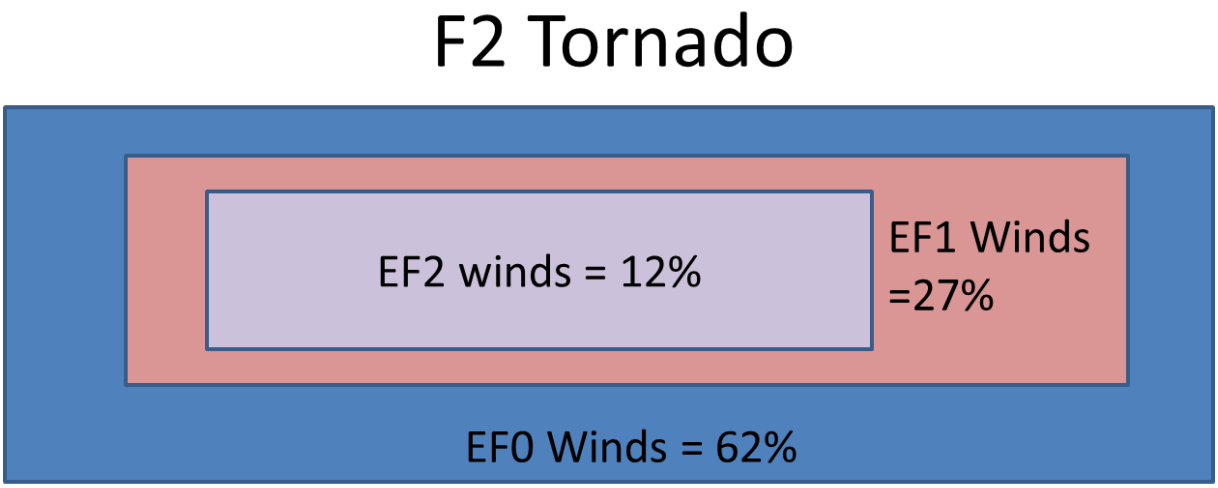

Figure 3.4 Schematic of the relative areas within a typical F2 tornado that experience EF0 or greater winds.

b. Data Processing

Correction for Tornado Misclassification

As stated previously, tornado magnitudes are estimated subjectively, given the degree of the damage. Any tornado dataset must therefore address tornado misclassification – instances in which observers estimate (and record) a tornado as being of one magnitude when, in reality, another would be more appropriate. A process for correcting the database for misclassification was developed by Lu (1995), who assumed that the tornado magnitude can be represented as a continuous, normally distributed variable, with a degree of overlap between categories. The estimated area of overlap allows for the calculation of a probability matrix that a tornado recorded at one magnitude should be reclassified as another (Table 3.4). An example is shown in Fig. 3.5 for both the F and EF tornado areas, where some F/EF1-3 tornado areas have been reassigned to the F/EF0, 4, and 5 categories. The total F0 area is therefore recalculated as .8413 F0 + .1574 F1 +…. Note that, after the correction for misclassification, category 5 tornado data now exists in the record, and this will be used to estimate the probability of F (or EF) category storms occurring in the future. This effective extrapolation of tornadic frequency is the sole source of F5 and EF5 tornadoes in our two-state record.

Table 3.4 Matrix to reassign recorded F tornado areas to corrected F categories. (from Lu (1995)). The same data is applied to correct for EF misclassification as well.

Recorded F Value

Corrected Fraction	0	1	2	3	4	5
0	0.8413	0.1574	0.0013	0	0	0
1	0.1574	0.6826	0.1574	0.0013	0	0
2	0.0013	0.1574	0.6826	0.1574	0.0013	0
3	0	0.0013	0.1574	0.6826	0.1574	0.001
4	0	0	0.0013	0.1574	0.6826	0.157
5	0	0	0	0.001	0.159	0.841

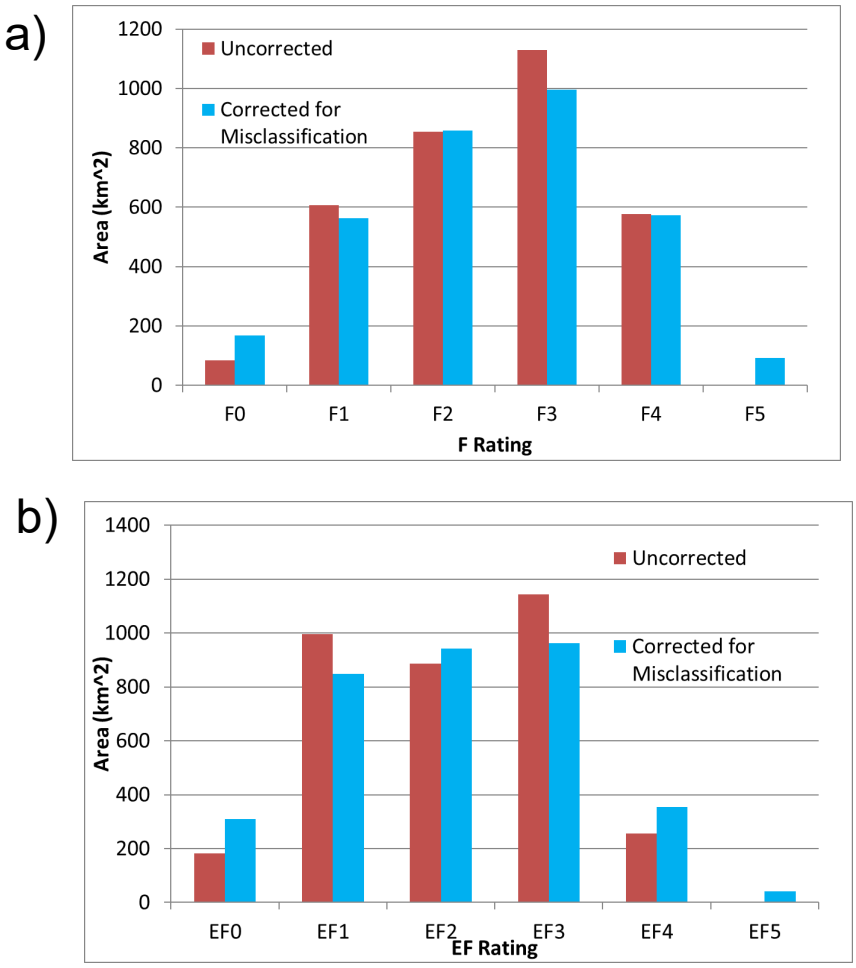

Figure 3.5 Total area (in SC and GA) covered by each category for the raw SPC data, and corrected for misclassification for the a) F-rated and b) EF-rated tornadoes.

Calculation of Total Tornado Area

The best way to calculate the total area covered by each F/EF category must also be considered. This can be done by simply adding the areas of the individual tornadoes (an arithmetic mean). R07, however, points out that it would be more accurate to assume that the tornado areas in the database do not constitute the entire 'universe' of tornado data, but were instead drawn from a lognormal distribution that accurately describes that universe. If we use the existing data to calculate the properties of that distribution, we could get a more accurate 'expectation value' – the expected area of a randomly selected tornado. Simply assuming that the arithmetic average is a good value to use as the expectation value can result in a biased tornado area.

R07 summarizes a procedure to estimate the expected area E(F) for each F category. We assume areas are lognormally distributed – the logarithm of the area (not the actual area) is normally distributed within category F. If we first take the natural logarithm of each tornado area $a(F,i)$ in category F, then get the mean u(F) and variance v(F) of that normally distributed variable:

$$u(F) = \frac{1}{N_F}\sum_{i=1}^{N_F} \ln\left(a(F,i)\right) \quad (5a)$$

$$v(F) = \frac{1}{N_F-1}\sum_{i=1}^{N_F} \left(\ln\left(a(F,i)\right) - u(F)\right)^2 \quad (5b)$$

then the mean area, E(F), is calculated as:

$$E(F) = e^{\left(u(F)+\frac{v(F)}{2}\right)} \quad (6)$$

This quantity, multiplied by the number of tornadoes in category F, is used to get a more accurate value of the total area A(F). Applied to the SPC data (and calculated for F and

EF separately), we get a new distribution of areas A(F) (Fig. 3.6) that is quite different from the original distribution. Not only are the total areas using the lognormal distribution larger than the total areas using the arithmetic mean, but the distribution is skewed more to the larger magnitudes.

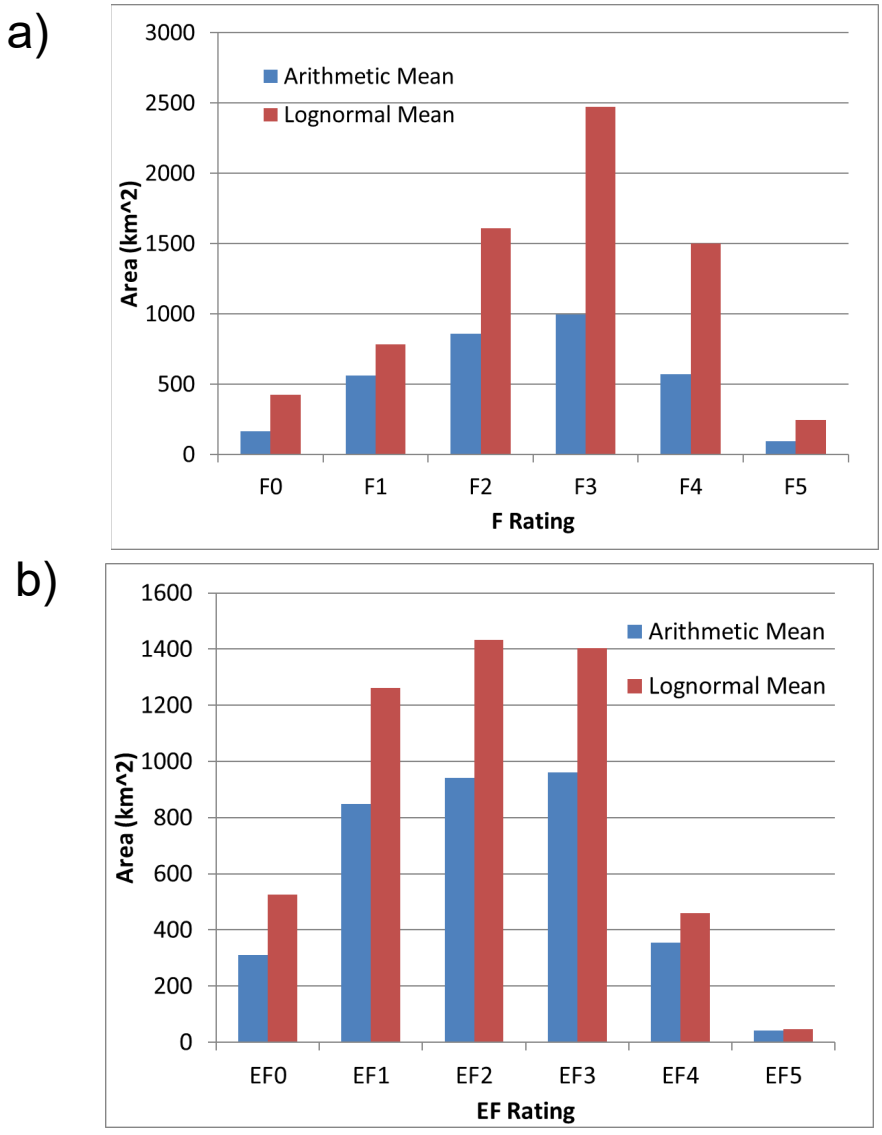

Figure 3.6 Total area (SC+GA) covered by each category for the raw SPC data calculated using the arithmetic mean (blue) and lognormal expectation value (red) for the a) F-rated and b) EF-rated tornadoes.

Correction for Reporting Bias

Changes in the observing networks, methods, and practices over time will lead to changes in the data that are recorded. The trend in F0/EF0 tornado occurrence after 1990 (but not others) (Fig. 3.2) suggests that these tornadoes were often missed in the past, and only in the later years do the reports capture their true statistics. R07 outlines a simple procedure to correct for this – assume that the statistics of the later years are representative of the entire interval, and adjust the values of E(F=0) and A(F=0) accordingly.

A Student's t-test reveals that the mean for the number of F0 tornadoes reported in the last 8 years of F-scale recording (1999-2006, the last 8 years that scale was applied) is significantly different from the previous years at an α= 1% level of significance (and the other categories were not), so we will apply this adjustment to only that category – for F=0, u(F) and v(F) are calculated only with data from 1999-2006 and E(0) is calculated as in Eq. 6. The number of F0 tornadoes is then rescaled for the entire 73-year record – the number that occurred from 1999-2006 is multiplied by 57/8 (1950 to 2006 = 57 years, 1999-2006 = 8 years), so that the average number per year for 1999-2006 is assumed to have occurred each year from 1950-1998. (The EF0 tornadoes are counted normally.)

Scale Conversion

To apply Table 3.3, we need a way to 'convert' each recorded EF-scale tornado area to a corresponding F-area. This is accomplished with the same method Lu (1995) applied to estimate the probability that a tornado recorded at one rating should actually be reclassified as another. We assume a probabilistic distribution for each EF category, centered at the category midpoint and with a standard deviation of half the width of each category (e.g., 10mph for the EF0 range of 65mph-85mph). This is used to calculate the probability that winds within each EF category lie within the ranges of the F categories (Table 3.5). (For example, ~62% of the total recorded EF0 area is reassigned as F1, while 38% is assigned as F0. The total F0 is then equal to 0.38 EF0 + .020675 EF1 +…)

Table 3.5 Matrix to reassign recorded EF tornado areas to the F categories.

F Value \ EF Value	0	1	2	3	4	5
0	0.38	0.020675	0	0	0	0
1	0.618	0.856	0.200	0.0057	0	0
2	.00011	.123	0.797	0.698	0.081	0.037
3	0	0	0.0023	0.297	0.838	0.146
4	0	0	0	0	0.08	0.325
5	0	0	0	0	0	0.478

Recorded Path Width

Finally, an important change in the tornado recording protocol was implemented in 1994 – the path width was recorded as the maximum width, rather than the mean width that had been estimated earlier. This will manifest itself as larger tornado footprint areas in later records, with correspondingly higher strike probabilities. In keeping with R07,

however, we elect to apply no correction to compensate for this, preferring to maintain conservative results.

The complete algorithm is outlined below and is applied separately to i) the two-state domain comprising Georgia and South Carolina using SPC data from 1950-2022, ii) the 1950-2022 period over a 2° x 2° domain centered at SRS using SPC data, iii) the 1950-2011 period over a 2° x 2° domain centered at SRS, using the data from W2013, and iv) the 1950-2011 period over a the two-state domain centered at SRS, using the data from W2013.

i) Calculate the mean u(F), u(EF), and variance v(F), v(EF) of the logarithm of the tornado areas within each F/EF category and count the number in each category N_F and N_{EF}. For F=0, only use the years 1999-2006 to get the means and variances and value of N_F.

ii) Calculate the expected tornado areas within each F/EF category according to Eq. 6.

iii) For F=0, rescale the number of tornadoes $N_{F=0}$ by multiplying by 57/8.

iii) Calculate the total area of each category as A(F) = E(F) x N_F, A(EF) = E(EF) x N_{EF}.

iv) Apply the misclassification matrix (Table 3.4) to adjust the area of the different categories for both F and EF.

v) Apply the EF-F allocation matrix (Table 3.5) to the EF areas to rescale them to the F categories.

vi) These areas are then used in Eqs. 3 and 2 to get the annual strike probability, and in Eq. 4 (Table 3.3) to get the probability of each wind speed, given that a strike occurs. The product of these two is then used to calculate the annual probability of a point experiencing winds above a threshold.

3.3 Results for Tornadoes

For the two-state domain, the total affected area A_T is 12,166 km^2, and the total area of the two-state domain A_R is 236,840 km^2, with a record length of N_{year}=73 years. Eq. 2 therefore yields a strike probability (the probability at each location in the domain that it will be within a tornado path) of 7.04 x 10^{-4} per year (Table 3.6). A full 2° x 2° domain covers an area of about 41,200km^2, but W98 applies a slightly smaller 'effective' area of 40,374 km^2, which we will apply here as well. Within that domain, the value of A_T is 2,704 km^2, for a larger strike probability of 9.18 x 10^{-4} (Table 3.6). When we limit the calculation to years before 2012 (as was done in W2013), we can see what changes exist in these values compared to those calculated at the time of the previous report (Table 3.6). (Note: The 1950-2011 values were recalculated to account for errors in the original dataset.)

Table 3.6 Calculated strike probabilities (per year).

Data Set	Strike Probability
Two-State Domain 1950-2022	7.04E-04
Two-State Domain 1950-2011	6.61E-04
2° x 2° Domain 1950-2022	9.18E-04
2° x 2° Domain 1950-2011	8.31E-04

Within the 2° x 2° domain, the SPC data has tornadoes occurring at a slightly higher frequency than the larger 2-state domain – the area of the latter is about 5.9 times larger, but has only about 5.7 times the number of tornadoes in the record. This is largely due to the low-frequencies in coastal areas (Fig. 3.1b,c) which skews the larger domain to slightly smaller frequencies. The total recorded tornado areas divided by tornado number for the smaller domain tend to be slightly larger, implying that a single tornado in the 2° domain will cover a larger area than is typical for the 2-state domain. These two effects combine for the larger strike probability in the 2° domain. Also, the average number of tornadoes per year is slightly higher in the current database than in the 1950-2011 data record, for a higher strike probability for both domains (Table 3.6).

Table 3.7a lists the probability of a point experiencing winds at each EF category, given that a strike occurs as determined by Eq. 4. For the 1950-2011 data (Table 3.7a), the probability is slightly weighted towards the higher categories (relative to the 2023 data) (Fig. 3.7a), with winds more likely to be in the EF3-5 range. In keeping with Fig. 3.7a, cumulative probabilities for the 1950-2023 data fall off faster than those for the 1950-2011 dataset (Fig. 3.7b). The probability per year that any point within the domain will experience tornadic winds at or above each threshold (Table 3.7b, Fig. 3.7c) is slightly higher for the 1950-2011 data than for the 1950-2023 data at the higher levels. The probabilities are higher in the 2° x 2° domain than for the 2-state domain at the lower thresholds, with higher probabilities in the larger domain for winds above 166mph.

Table 3.7 a) Probability of a point within a given tornado experiencing winds at the indicated speeds. b) Probability per year of a specific point in the respective domain experiencing winds at or above the indicated speeds.

a)

Wind Speed (mph, 3 s gust)	SPC 2-State domain 1950-2022	SPC 2° x 2° Domain 1950-2022	2-State domain 1950-2011	2° x 2° Domain 1950-2011
65	0.6338	0.6362	0.6262	0.6511
86	0.2415	0.2438	0.2411	0.2368
111	0.0924	0.0932	0.0961	0.0851
136	0.0268	0.0228	0.0300	0.0223
166	0.0048	0.0033	0.0059	0.0040
200	0.0004	0.0003	0.0004	0.0003

b)

Wind Speed (mph, 3 s gust)	SPC 2-State domain 1950-2022	SPC 2° x 2° domain 1950-2022	2-State domain 1950-2011	2° x 2° Domain 1950-2011
65	7.04e-4	9.17e-4	6.61e-4	8.31e-4
86	2.58e-4	3.33e-4	2.47e-4	2.90e-4
111	8.75e-05	1.10e-4	8.75e-05	9.28e-05
136	2.25e-05	2.42e-05	2.40e-05	2.21e-05
166	3.65e-06	3.24e-06	4.17e-06	3.58e-06
200	2.63e-07	2.30e-07	2.92e-07	2.45e-07

The EF-speeds for the two-state domain (using all years) are plotted against their respective return periods - the expected time until a specified threshold is exceeded (Fig. 3.8), and an exponential fit shows the winds associated with *any* return period (Table 3.8) (as required by DOE-STD-1020-2016, Section 4.3.2.4 and 4.3.2.5). Any point within the SRS domain can expect tornadic winds of about 64 mph every 1000 years, and winds of 262 mph every 10^8 years.

ANS-2.3-2011 lists the results of a PHA for tornadic winds in which the continental United States is subdivided into three broad regions, and separate statistics are calculated for each. The SRS lies within Region I (their Figure 1), which encompasses Illinois, Arkansas, Missouri, Illinois, Iowa, and large parts of Texas, Oklahoma, Kansas, and Nebraska, which are all known to have heavy tornado activity. Table 3 of their report lists wind speeds of 170mph for a return period of 10^5 years, 200mph for 10^6 years, and 230mph for 10^7 years (Fig. 3.8). The corresponding values for our current analysis (calculated over the 2-state domain, and based on the extrapolation in Fig. 3.8) are 144mph, 183mph, and 223mph, respectively, for those same periods, which is slower than those calculated over the larger, more active domain as expected.

Additionally, DOE (DOE-STD-1020-2016) guidelines (Section 4.3.2.4) require tornadic wind speeds for 2 return periods – 50,000 years (corresponding to wind design category 3 (WDC-3)) and 125,000 years (WDC-4), and these are listed in Table 3.9 (also based on extrapolation).

a)

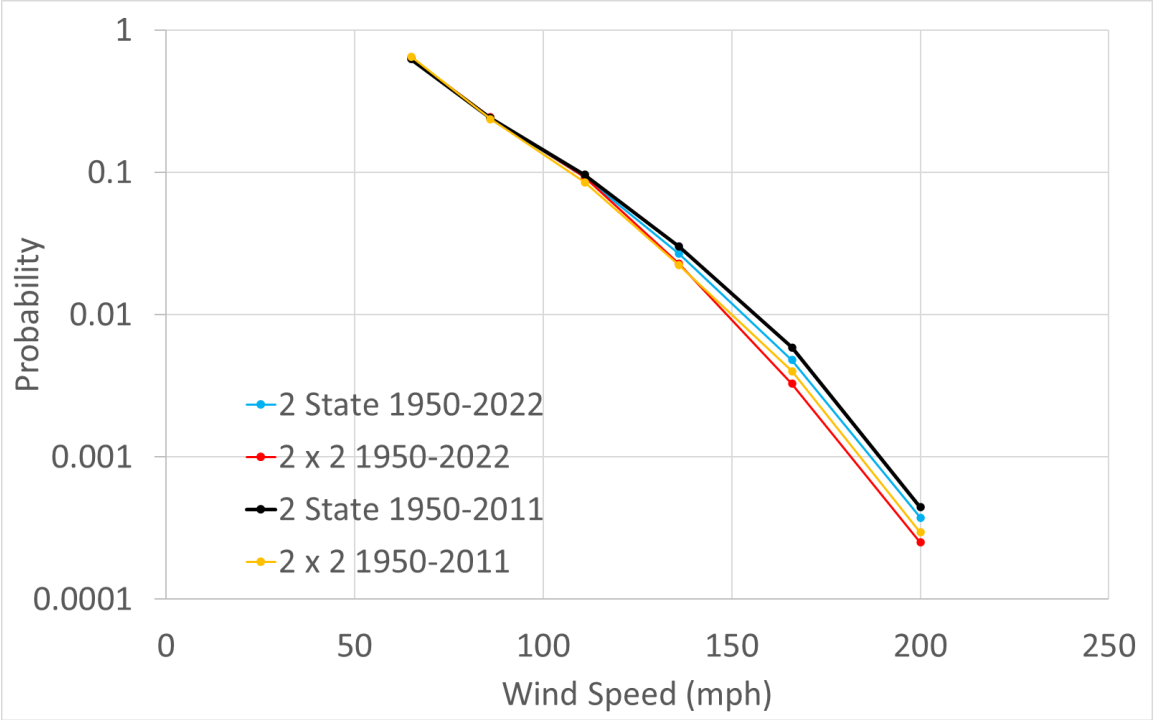
1
0.1
0.01
0.001
0.0001
Probability
2 State 1950-2022
2 x 2 1950-2022
2 State 1950-2011
2 x 2 1950-2011
0
50
100
150
200
250
Wind Speed (mph)

b)

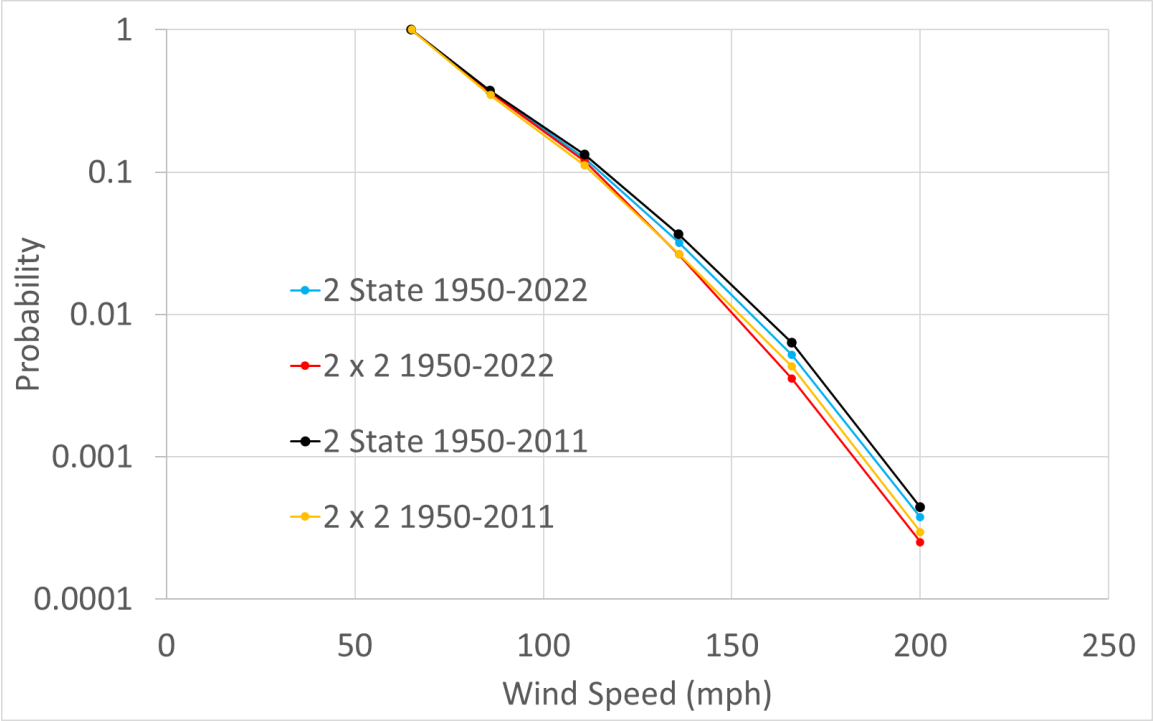
1
0.1
0.01
0.001
0.0001
Probability
2 State 1950-2022
2 x 2 1950-2022
2 State 1950-2011
2 x 2 1950-2011
0
50
100
150
200
250
Wind Speed (mph)

c)

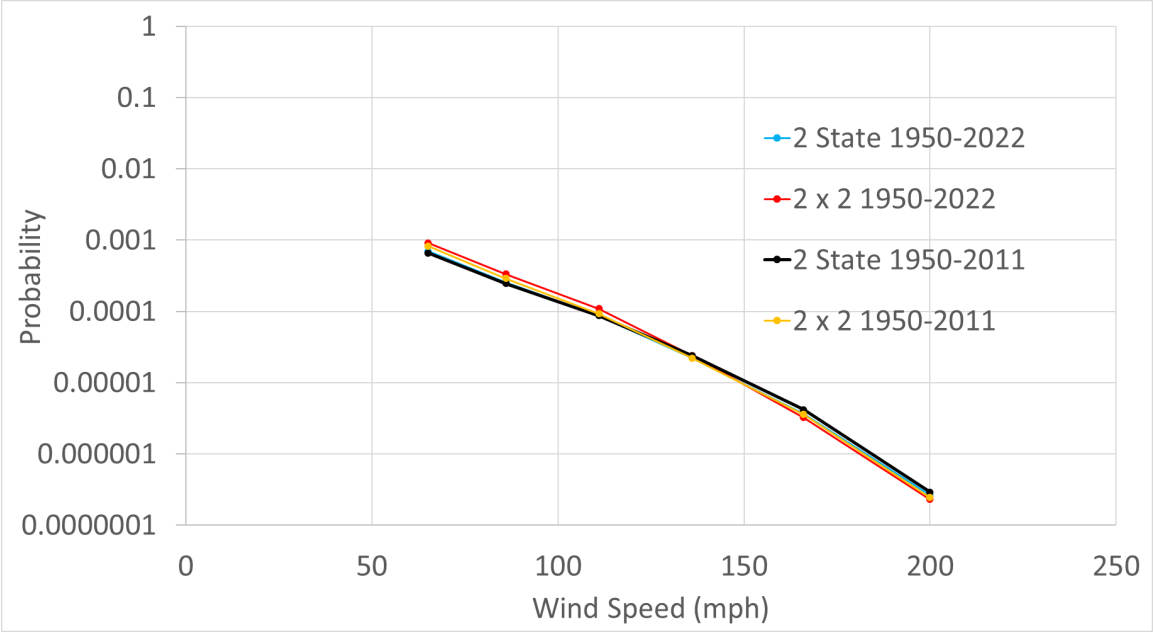

Figure 3.7 a) The probability a point within a tornado path will have winds (3 second gust) at the given velocity, given that a strike occurs, b) the cumulative probability that any point within a strike will experience winds at or above that threshold, c) the probability (per year) that any point will experience winds at or above the given threshold.

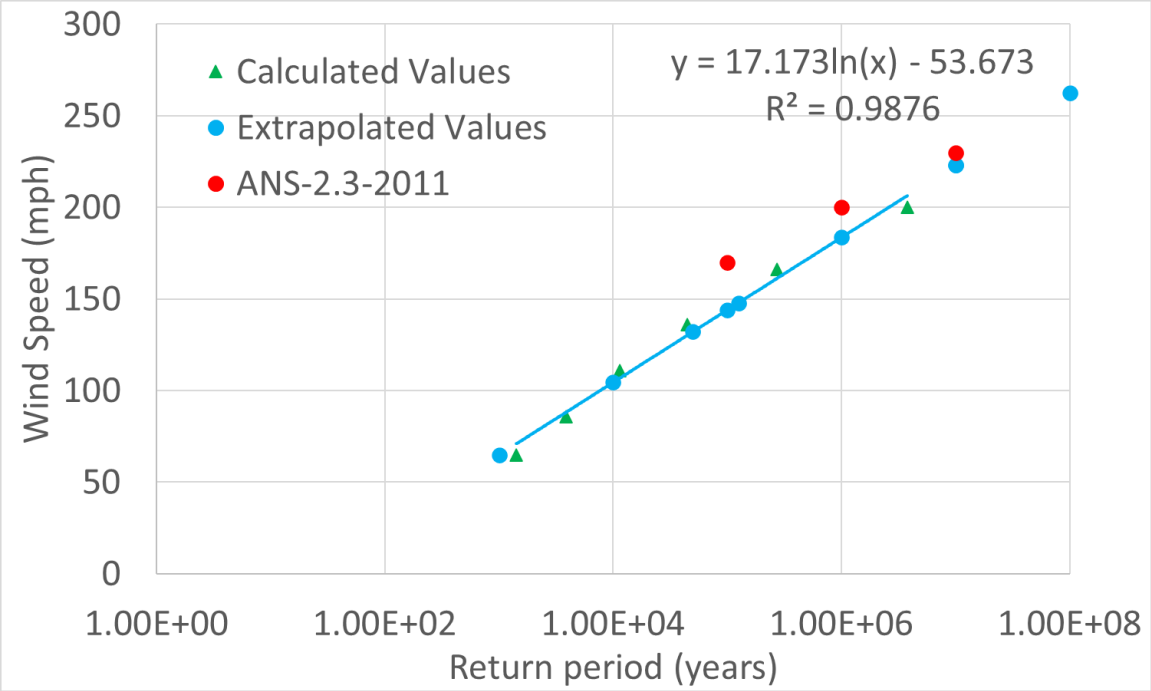

Figure 3.8 Tornadic wind speeds for the 2-state domain (using all years) corresponding to various return periods for both the values calculated from the observed tornadic wind speeds (with Eqs.1-4) (3 second gust), for a linear extrapolation of those values, and values from the ANS-2.3-2011 report (also based on extrapolation).

Table 3.8 Expected wind speeds for various return periods.

Return Period (years)	Wind Speed (mph, 3 second gust) Two-State Domain	Wind Speed (mph, 3 second gust), ANS-2.3-2011
1E+03	65	110
1E+04	104	140
1E+05	144	170
1E+06	183	200
1E+07	223	230
1E+08	262	260

Table 3.9 Tornadic wind speeds for DOE-mandated return periods, based on the extrapolation.

Return Period (years)	Wind Speed (mph, 3 s gust) Two-State Domain	Wind Speed (mph, 3 s gust), ANS-2.3-2011
50,000 (WDC-3)	132	161
125,000 (WDC-4)	147	173

4.0 Straight-Line Winds

DOE-STD-1020-2016, Section 4.3.2.4 requires that sites develop a wind-related hazard curve (i.e., wind speed at the site as a function of return period in years), according to ANS-2.3-2011. The ANS standard (ANS-2.3-2011, Section 3.4.2) specifies that a Fisher-Tippet Type I distribution be applied to estimate the wind risk probabilities for straight-line winds, but allows for the possibility of other, more suitable distributions if they can be demonstrated to be more applicable. Eliasson (1997) outlines a procedure for calculating the probability of extreme events by applying extreme value theory – the process of using existing data to create a probability function, then 'reading' the values at the tail of the function, which represent the largest, least likely values. As in W2013, we adapt Eliasson's (1997) algorithm, as well as that of Hosking et al. (1985), for our purposes here, applying it to the longer datasets now available.

4.1 Wind Data

National Weather Service (NWS) wind gust data were analyzed for four sites in the vicinity of SRS: Augusta, GA, Macon, GA, Columbia, SC, and Athens, GA. Additionally, wind gust data were collected and analyzed from the CLM site near the center of SRS. Table 4.1 lists the locations and record lengths of the 5 sites. NWS wind gusts are defined as the peak three-second wind speed within each hour (Smith et al., 2013). Data were recorded over a period of five decades, allowing for a reasonable sample from which to derive the statistics.

Table 4.1 Wind station data, including mean and standard deviation of the annual maximum wind gusts at SRS and the NWS stations.

Station	No. of years	Mean Gust Speed (mph)	Std. Deviation of Gust Speed (mph)
Athens	50 (1973-2022)	49.82	9.60
Augusta	50 (1973-2022)	52.42	7.98
Columbia	50 (1973-2022)	54.32	9.03
Macon	50 (1973-2022)	57.18	13.25
CLM	33 (1990-2022)	55.90	11.65

To be recorded as a gust, an NWS wind reading must be sustained for either five seconds when recorded with an anemometer (prior to 2003), or for three seconds if recorded with an ultrasonic device (generally after 2003) (Smith et al., 2013). (The shorter period is the minimum required by ANS-2.3-2011, Section 3.4.1). Little difference was seen in wind speeds before and after instrument transitions were made (Smith et al., 2013), thus we did not correct for this. Wind recorded at CLM is somewhat different – the 1Hz cup anemometer saves data in 1 second blocks, and prior to March of 2014 *any* wind maximum within a 15-minute interval is recorded as the 'gust' reading for that time block. (After that time, a sonic anemometer was installed, and the standard was increased to 3s.) In practice, however, recorded gusts rarely last less than 1 second. This still allows fast but brief wind gusts to enter the record that are different from criteria at an NWS station, skewing the typical gust to be higher at CLM. A correction exists for this, but for now we will first apply the algorithm to the data as is with the caveat that the wind gusts at the site tower are defined differently than at the NWS stations. A comparison of one-second SRS wind gust data to the NWS three-second data shows the former to not be out of line with the latter (Table 4.1), so we do not believe that we are introducing a great error to the statistics.

Another issue with the CLM data is that the anemometer is at four meters (since 1993, and at 2m prior), while the standard for NWS stations is ten meters. This would cause the CLM data to have slower recorded speeds than the other stations (all else being equal). Using CLM wind data at four meters and from a second anemometer on the tower at 18 meters, we apply a logarithmic correction (accounting for the 2m to 4m shift) to obtain an estimate of the ten-meter wind at the Climatology tower location (as per DOE-STD-1020-2016, Section 4.2.3.2b).

One problem exists with the NWS wind data: for pragmatic and economic reasons, the 10m standard was not always followed (Weber, 2002). For the stations selected, the height tended to lie within the range of 6m to 11m. The 10m standard was not met until the mid-1990s. This would leave us with two fewer decades of data if we eliminated all data prior to this time, nor is a realistic correction possible with readings at only one level, so we elected to use this data as is. A time series of wind gusts does not show an obvious trend or change in variability at the time of the transition, so we do not believe that we are introducing any large error to the analysis.

We will use the NWS and CLM data to establish a relationship between the wind speed and the probability that such speeds have occurred (or will occur) in the vicinity of SRS. We will first determine the statistical properties of various candidate functions, then select the one that best fits the data. Our goal is to calculate the expected maximum wind gust within a one-year period for various return periods, and we therefore require the annual maxima that have occurred. Following the strategy outlined by Eliasson (1997), the maximum wind speed from station (j) in year (i) is (x_{ij}) (e.g., Fig. 4.1a).

Since the number of years available at any one station is usually insufficient to investigate the nature of the maxima, Eliasson (1997) regionally pools the data from multiple observation stations. The maxima data from each time series are standardized by subtracting the station mean ($\bar{x}_j$) and then normalizing by the station standard deviation (s_j) of the maximum wind gusts for station (j) (Fig. 4.1b):

$$\tau_{ij} = \frac{X_{ij} - \bar{X}_j}{s_j} \quad (7)$$

resulting in n_j standardized wind deviations for station *j*, (*j* = 1, 2, ..., *k*). There are now several (*k*) series of length n_j (one for each station *j*), each with zero mean and a standard deviation of one. These values of τ_{ij} represent the collection of *all* standardized wind deviations (all stations for all years), and we can use them to determine the shape of the distribution from which they were drawn. The goal then is to calculate the probability of *any* value of τ_{ij} occurring, based on how well the distribution fits one of several probability curves.

The τ_{ij} values from all stations are pooled together and then sorted from smallest to largest. Label the first (smallest) τ_{ij} value in this sequence as $\tau_{(1)}$, the next (second smallest) τ_{ij} value in this sequence as $\tau_{(2)}$, and so on where the largest of the τ_{ij} values in this sequence is $\tau_{(n_T)}$, where $n_T = \sum_{j=1}^{k} n_j$ are the total number of observations at all of the stations (Fig. 4.2).

a)

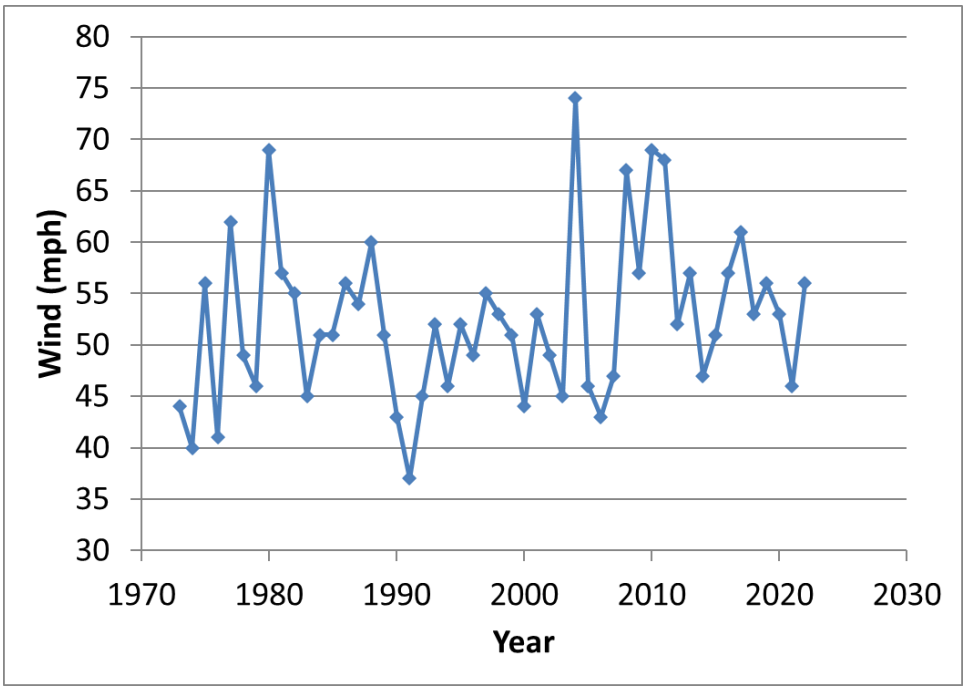

b)

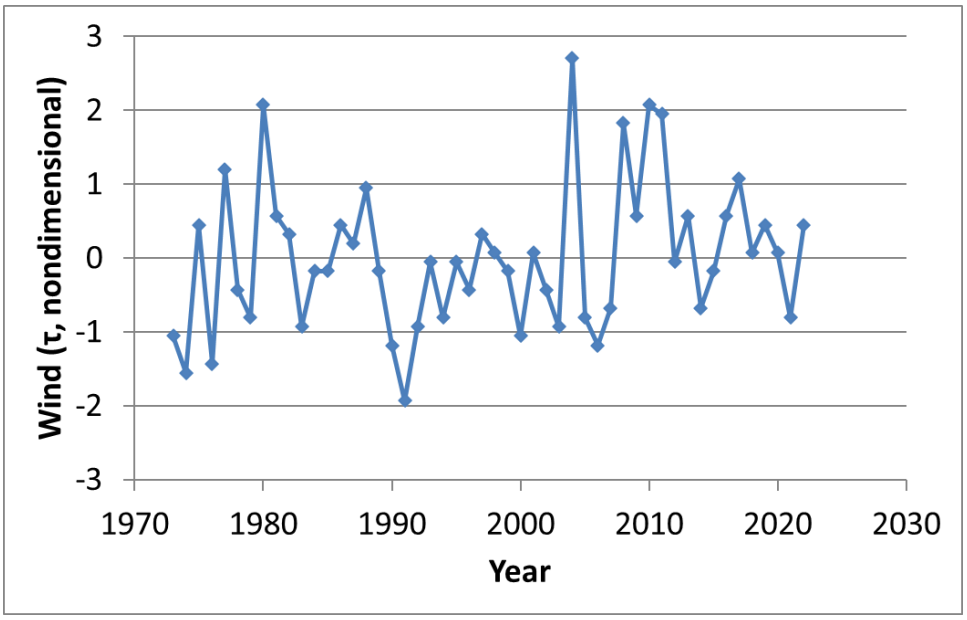

Figure 4.1 a) Annual wind gust maxima each year at Augusta, GA (NWS). b) As in a) but rendered nondimensional with the mean removed and normalized by the standard deviation (Eq. 7).

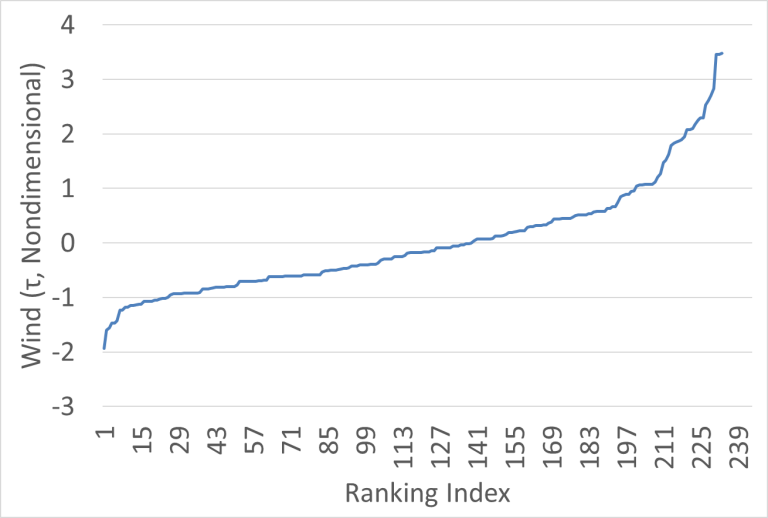

Figure 4.2 Ranked values of normalized wind maxima τ_{ij}.

4.2 Extreme Value Theory

The Fisher-Tippet, also known as generalized extreme value (GEV), distributions play an important role in modeling return periods for maxima based on long series of observations. The GEV distribution will be fit to the pooled standardized annual maximum wind deviations ($\tau_{(1)}, \tau_{(2)}, \ldots\ldots \tau_{(n_T)}$). From Hosking et al. (1985), the maximal GEV cumulative distribution function (CDF) (probability a randomly selected value is below τ) is:

$$F(\tau;\xi,\alpha,\kappa) = \begin{cases} exp\left\{-\left[1-\kappa\left(\frac{\tau-\xi}{\alpha}\right)\right]^{1/\kappa}\right\}, \kappa \neq 0 & \text{(8a)} \\ exp\left\{-exp\left\{\left(\frac{\xi-\tau}{\alpha}\right)\right\}\right\}, \ \kappa = 0 & \text{(8b)} \end{cases}$$

where ξ is a location parameter that determines an offset value of the data, α is a scale parameter that helps determine the range of the data, and κ is a shape parameter which determines the curvature of the CDF at the extreme values, as will be illustrated. The maximal GEV distribution can be partitioned into several special cases depending on the

value of κ (Fig. 4.3a): the GEV Type 1 (GEV1) distribution occurs when $\kappa = 0$, the GEV Type 2 (GEV2) distribution occurs when $\kappa < 0$, and the GEV Type 3 (GEV3) distribution occurs when $\kappa > 0$. The ordinate of the CDF plot (Fig. 4.3a) can be interpreted as the 'non-exceedance' probability; that is, the probability that a randomly selected deviation value will be at or lower than that specified value of τ in a given year. The value of the CDF monotonically increases as the specified value of τ increases, and experiencing wind values faster than τ becomes progressively less likely.

a)

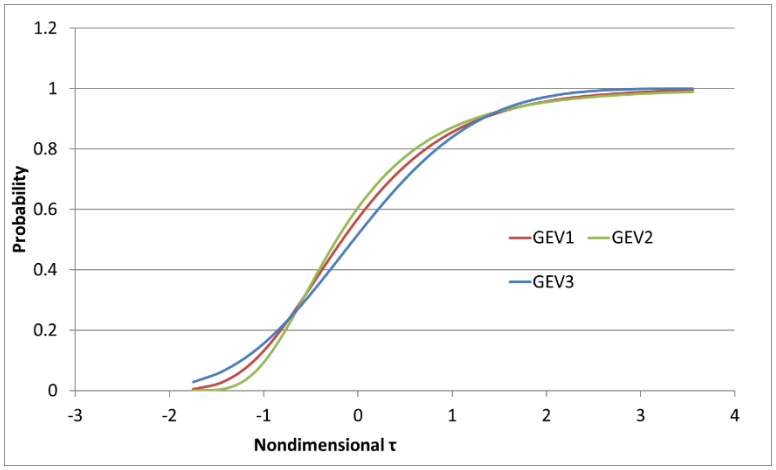

b)

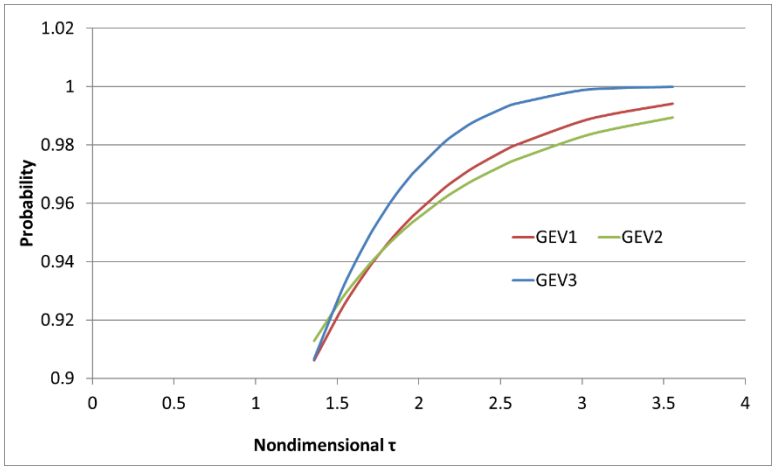

c)

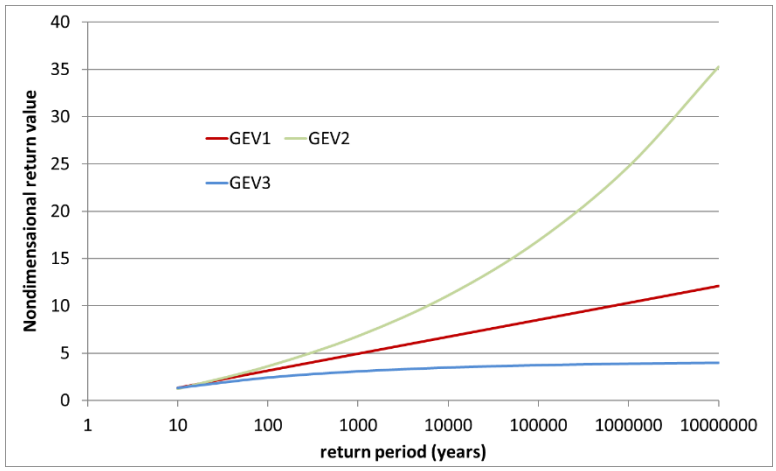

Figure 4.3 a) Nonexceedance probability curves for a GEV2 (κ < 0), GEV1 (κ = 0), and GEV3 (κ > 0) distribution. b) As in a), but above the 90th percentile. c) Return values for the three distributions.

At the extreme values (e.g., values of τ higher than 1.5), the GEV2 distribution has lower non-exceedance probabilities than the GEV1 (Fig. 4.3b), making it *more* likely we will exceed any such value for τ. Conversely, the GEV3 distribution has higher non-exceedance probabilities (Fig. 4.3b), making large extremes *less* likely than a GEV1 distribution.

We can also calculate quantiles; for example, what wind speed value of τ is 99% likely to *not* be exceeded in a given year? Solving Eqs. 8 for τ, the *p*-th quantile for the maximal GEV distribution can be determined by

$$\tau_p = \begin{cases} \xi + \alpha[1 - (-\ln p)^{\kappa}]/\kappa, \text{if } \kappa \neq 0 \\ \xi - \alpha \ln(-\ln p), \text{if } \kappa = 0 \end{cases} \quad (9)$$

where *p* is the probability of *not* exceeding a wind speed value of τ_p in a given year.

Let $p = F(\tau; \xi, \alpha, \kappa)$ be the probability of not exceeding the wind speed value τ in a given year. If 1 - *p* is small, and the probability of more than one such event in a short duration is negligible, the return period (the average time between successive events) can then be approximated by $RP_{\tau} \approx 1/(1 - p)$. For example, when *p* = 99%, the return period is approximately 100 years.

The GEV1 is the simplest of the three types, and its return value curve is a straight-line (Fig. 4.3c). The GEV2 distribution has lower nonexeedance probabilities than the GEV1 (Fig. 4.3b), and the return value curve is therefore concave upward, yielding higher return values for any return period (Fig. 4.3c). Conversely, the GEV3 distribution has

higher nonexceedance probabilities (Fig. 4.3b) and the return period curve is concave downward. This distribution will therefore yield *lower* return period values (Fig. 4.3c).

One thing to note from both distributions – there is a limit to the range at which they should be applied, beyond which an unchanging maximum should instead be applied (Eliasson, 1997). To be conservative, however, we elect instead to report the values as calculated.

The proper distribution is determined by first calculating the parameter (κ) that dictates the shape of each curve, and evaluate which one fits the data best. A technique for estimating κ by Hosking et al., (1985) is based on an approximate solution to a set of 'probability weighted moments' (PWM). The sample PWMs are as follows (Hosking et al., 1985):

$$b_0 = \frac{1}{n_T}\sum_{i=1}^{n_T} \tau_{(i)} \quad (10a)$$

$$b_1 = \frac{1}{n_T(n_T-1)}\sum_{i=1}^{n_T}(i-1)\tau_{(i)} \quad (10b)$$

$$b_2 = \frac{1}{n_T(n_T-1)(n_T-2)}\sum_{i=1}^{n_T}(i-1)(i-2)\tau_{(i)} \quad (10c)$$

and the PWM estimator of κ is the solution to the following non-linear equation:

$$(3b_2 - b_0)/(2b_1 - b_0) = (1 - 3^{-\kappa})/(1 - 2^{-\kappa}). \quad (11)$$

An exact solution of Eq. 11 requires an iterative process. To avoid such an iterative solution, Hosking et al. (1985), notes that the right side of Eq. 11 is almost linear for -0.5

< κ < 0.5. With this assumption, Hosking et al., (1985) derives the following approximate estimators:

$$c = \frac{2b_1 - b_0}{3b_2 - b_0} - \frac{ln2}{ln3} \quad (12)$$

$$\kappa = 7.859c + 2.9554c^2 \quad (13)$$

According to Hosking et al., (1985), the estimated value of κ from Eq. 13 can be judged by how well it satisfies the original non-linear Eq. 11. When using Hosking's linear approximation, the resulting error in κ is less than .0009 through the range -.5 < κ< .5 when compared to the iterative (exact) solution.

The estimated value of κ is used to determine which type of extreme value distribution to apply. Values close to 0 are indicative of the GEV1 distribution
(Eq. 8b), while values further away carry progressively less support. Deciding on which to use can be difficult as the existing data can be seen to fit either distribution equally well (Fig. 4.4a, b). According to Hosking et al., (1985), we can calculate a Z-statistic and determine an approximate 95% confidence interval for κ:

$$Z = \kappa\sqrt{\frac{n_T}{0.5633}} \quad (14)$$

W98 sets a range of -1.96 < Z < 1.96 to indicate that κ is not significantly different from 0.

Another approach to identifying which special case of the GEV is applicable is to compare the probability values calculated assuming a particular limiting case against

probabilities inferred from the $\tau_{(i)}$ data series. First, Eqs. 8 are set to p, and then linearized as

$$-\ln(-ln(p)) = \frac{\tau_{(i)}-\xi}{\alpha}, \text{for } \kappa = 0 \quad (15a)$$

$$-ln(p))^{\kappa} = (1 - \frac{\kappa(\tau_{(i)}-\xi)}{\alpha}), \text{for } \kappa \neq 0 \quad (15b)$$

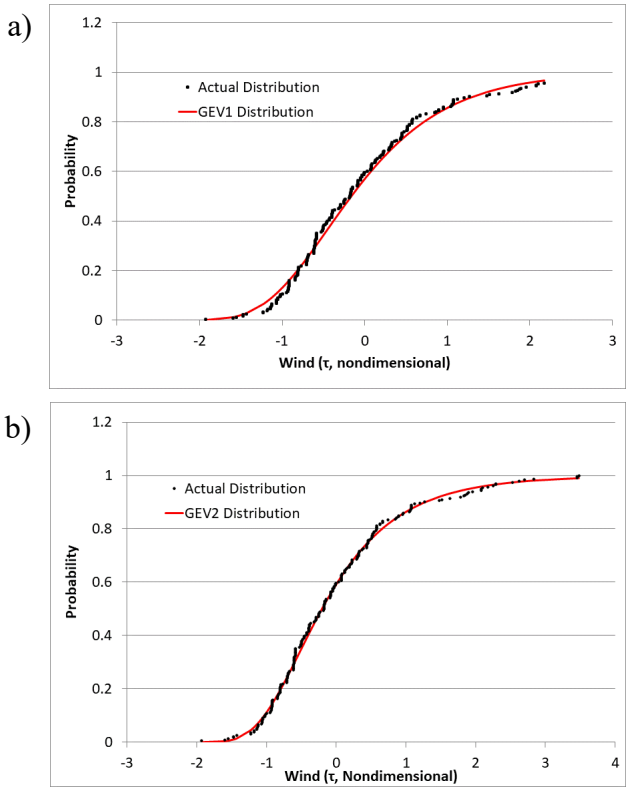

Figure 4.4 Comparison of the actual wind gust data distribution with the a) GEV1 and b) GEV2 distributions, calculated using Eq. 15a and 15b, respectively.

A calculation of both the (theoretical) left-hand side (LHS) and the (actual) right-hand side (RHS) for the Eqs. 15 values, and the correlation (r^2) between them, is the primary tool used in this report to select which of the two distributions will be used (Fig. 4.4) to calculate the probabilities.

To do the comparison, we first need to calculate both distributions (that is, solve Eqs. 8) by calculating their respective parameters. To calculate the GEV1 ($\kappa = 0$) distribution the parameters ξ and α are set to constant values (α =.779697, ξ=-.45004) (Eliason, 1997). For $\kappa \neq 0$, we instead calculate ξ and α using the following equations from Hosking et al., (1985):

$$\alpha = \frac{(2b_1 - b_0)\kappa}{\Gamma(1+\kappa)(1-2^{-\kappa})} \quad (16a)$$

$$\xi = b_0 + \alpha\{\Gamma(1+\kappa) - 1\}/\kappa. \quad (16b)$$

The curves in Eq. 8 represent two theoretical CDFs. We relate the probability of nonexceedance of τ_p (e.g., 95%) to its corresponding return period (e.g., RP_{τ_p} = 20 years):

$$Prob\left(T_{\tau_p} => RP_{\tau_p}\right) = F(\tau_p) = \left(1 - \frac{1}{RP_{\tau_p}}\right) \quad (17)$$

For any RP_{τ_p} we solve Eq. 8a or Eq. 8b for τ, using the values of ξ and α, and then restore the standard deviation and mean for each station according to the method outlined in Eliasson (1997). W98 outlines two procedures (one for κ=0, another for κ≠0) for calculating the value of τ_p corresponding to a return period P, and converting that value of τ_p to an actual wind speed value.

For a GEV1 distribution with a given return period RP_{τ_p}, the wind speed at Station *j* corresponding to a return period of RP_{τ_p} years is (W98):

$$X_{p_j} = s_j\left(-\ln\left[-ln\left\{\left(1 - \frac{1}{RP_{\tau_p}}\right)\right\}\right] - 0.57722\right)\left(\frac{1}{1.28255}\right) + \overline{X_J} \quad (18)$$

where the values 0.57722 and 1.28255 are from Eliasson (1997), $\overline{X_j}$ is the mean at that station, and s_j is the standard deviation.

When calculating the values of X_{p_i} for a set of stations, we can get a smoother fit by calculating the coefficients of variation of the respective stations (W98):

$$CV_j = \frac{s_j}{\overline{X_j}} \tag{19}$$

By defining $\overline{CV}$ as the average of CV_j values of all the *k* stations, W98 calculates the variable C_a as:

$$C_a = 0.78/\{\left(\frac{1}{\overline{CV}}\right) + 0.72\} \tag{20}$$

If we define X_{5j} as the 5-year return period value for a particular station *j* (calculated with Eq. 18), the wind speed value of X_{Pj} for any P value at j is then given as:

$$X_{Pj} = X_{5j}[1 + C_a(y - 1.5)] \tag{21}$$

where

$$y = -\ln\left(-\ln\left(1 - \frac{1}{RP_{\tau_p}}\right)\right) \tag{22}$$

If we must apply a GEV2 or GEV3 distribution, we must solve for Eq. 8a for the wind speed τ. This gives us the wind speed value X_{p_j} associated with a return period of RP_{τ_p} years at Station *j* (W98).

$$X_{p_j} = \overline{X_j} + s_j(\xi + (\frac{\alpha}{\kappa})\ (1 - y)) \tag{23}$$

where

$$y = \left[-\ln\left(1 - \frac{1}{RP_{\tau_p}}\right)\right]^{\kappa} \tag{24}$$

4.3 Results for Wind Gusts

The GEV1 distribution is commonly used to fit a CDF to a ranked dataset, but this assumes a value of κ=0. If the value deviates substantially from that, a GEV2 distribution would be more appropriate. We therefore require a method to decide which distribution to use, especially as the final values can be sensitive to the selected distribution. W98 accomplished this by applying a Z-score significance test (Eq. 14) to estimate if κ was significantly different from 0. For the current analysis, we consider both the Z-score and a fit of the data to both distributions using Eq. 15.

For the wind data, we obtain κ = -0.08388. We see in Fig. 4.5a,b that the GEV2 (κ≠0) distribution actually fits the data (slightly) better than the GEV1 (κ=0), implying that the former is a more reliable predictor for extreme wind gust values. However, the Z statistic is -1.70, well within the -/+1.96 threshold to be different from 0 at the 95% significance level. Therefore, we elect to use the GEV1 in our final analysis of this variable.

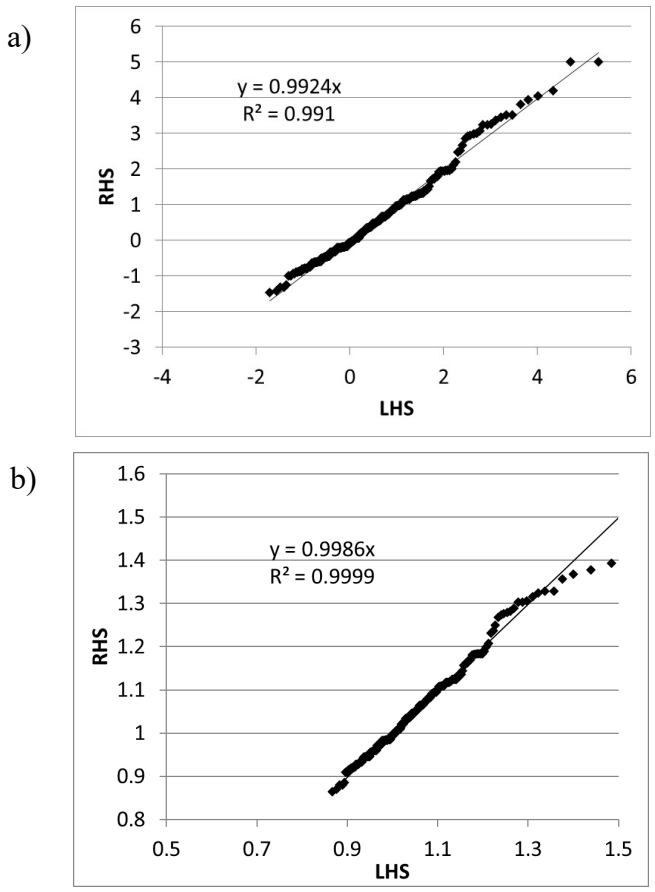

Figure 4.5 Comparison of the left hand side (LHS) and right hand side (RHS) of Eq. 15 for a) the GEV1 distribution, and b) the GEV2 distribution.

We then apply Eq. 21 to the data and solve for X_P for each station, restoring each respective mean and standard deviation. The results for SRS (Table 4.2, Fig. 4.6) show that we may expect a sustained gust of ~70mph every 10 years, with a gust of ~150mph every 100,000 years. These values are similar to those from the W2013 report (which also used the GEV1 distribution for wind speeds). The values from ANS-2.3-2011 (Table 3, Region 1) compare well with those from the current report (Fig. 4.6). We plot the SRS data along with the tornadic wind probabilities from Section 3 (Fig. 4.7). Wind

speeds for return periods less than about 100,000 years are actually faster for the straight-line winds (largely due to the fact that tornado strikes are rare and affect a small area), but for periods longer than that, tornadic winds represent a larger hazard. DOE guidelines (DOE-STD-1020-2016, Section 4.3.2.4) also require wind speeds for 2 return periods – 2,500 years (WDC-3), and 6,250 years (WDC-4), and these are listed in Table 4.3.

Table 4.2 Straight-line wind speeds for selected return periods.

Return Period (years)	Wind gust (mph), Current report	Wind gust (mph) from ANS-2.3-2011. The value for 100000 years is based on an extrapolation of the other values, which are listed in the report.
10	70.58	76
100	90.29	96
1000	109.65	118
10000	128.97	137
100000	148.28	158

Figure 4.6 Projected wind gust values for various return periods at SRS (from Eq. 21), along with the values from the ANS-2.3-2011 reports.

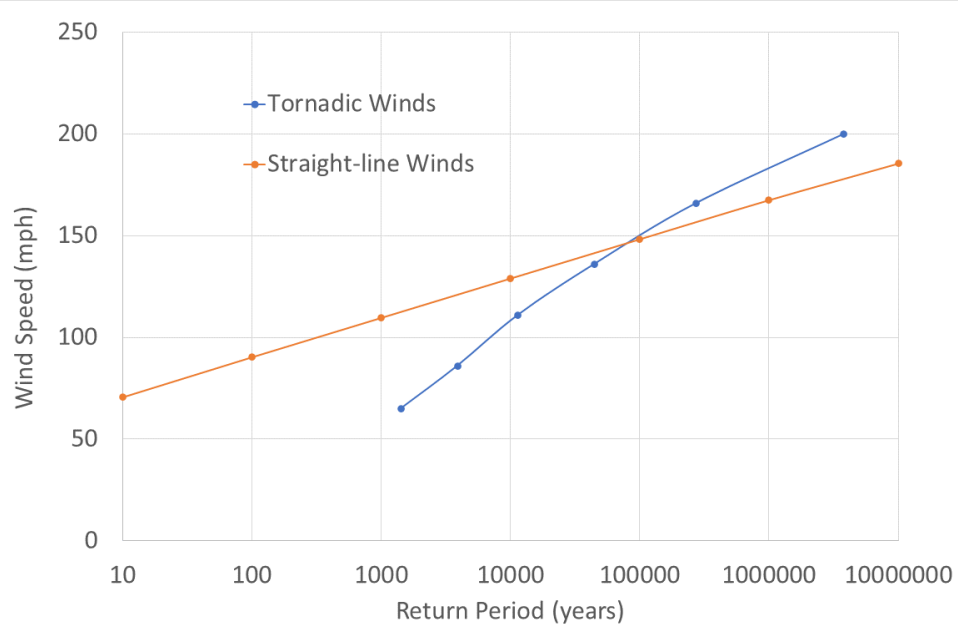

Figure 4.7 Comparison of tornadic (2-state) and straight-line wind gust probabilities.

Table 4.3 Straight-line wind speeds for DOE-mandated return periods.

Return Period (years)	Wind gust (mph)	Wind gust (mph) ANS-2.3-2011 (interpolated)
2500 (WDC-3)	117.34	125
6250 (WDC-4)	125.03	133

As mentioned previously, the definition of a 'gust' – how long a wind reading must last to be recorded – has not been kept constant in the SRS data. In March of 2014, the minimum was increased from 1 second to 3 seconds, which could create a bias by allowing brief winds before 2014 to remain in the record while eliminating equally brief readings after that time. A correction exists for this – multiply the older 1-second values by 0.959, implying that the lowered values approximate what was sustained for 3 seconds. The analysis was redone, and little change in the return period values was noted, so we do not believe this change has affected our results.

5.0 Precipitation

DOE-STD-1020-2016, Section 5.4.1.3 calls for ‘stochastic methods’ or ‘probabilistic hydrologic modeling’ to determine extreme precipitation frequency, and Section 7.4.1.1 again calls for the relationship between precipitation level and the associated return period in years. As with the straight-line winds, extreme precipitation probability thresholds will be calculated with the algorithm of W2013 – we will apply GEV1, 2, 3 distributions to the data, and ‘read’ the desired extreme values from the tails of the distribution. As before, we will start with a time series of the maximum precipitation total for each year, then calculate how likely *any* total is from that distribution. The relevant statistic with flood potential is how much rain falls within a specified amount of time (e.g., 6 hours), and we will calculate probabilities for various such accumulation periods.

5.1 Precipitation Data

We have assembled and collected precipitation data records from several locations, both on- and off-site. They were recorded at various intervals, and we must aggregate the data within each record to each desired accumulation period. On site, we have data recorded daily at twelve locations, with 15-minute data recorded at CLM (Table 5.1). We have also collected offsite NWS data from three regional weather stations, both every 15 minutes and hourly (Table 5.2).

Table 5.1 Precipitation Data at SRS. Data was collected over the period from 1964 to 2023.

Station	No. of years	Freq. of Observation
700-A	59	Daily
BARR2	51	Daily
BARR3	58	Daily
BARR5	47	Daily
100-C	38	Daily
400-D	49	Daily
200-F	55	Daily
200-H	38	Daily
100-K	38	Daily
100-L	43	Daily
100-P	54	Daily
SRTC	58	Daily
CLM (SRS)	22	15 Minutes

Table 5.2 National Weather Service precipitation data. Data was collected over the period from 1950 to 2023 for the hourly data and from 1971 to 2023 for the 15 minute data.

Station	No. of years	Freq. of Observation
Clark Hill	41	15 Minutes
Louisville	50	15 Minutes
Wagener	47	15 Minutes
Clark Hill	68	Hourly
Louisville	73	Hourly
Clark Hill	68	Hourly

The data – recorded at various intervals – must be aggregated to each desired accumulation period. We will use the same accumulation periods as in W2013 – 15 minutes, 1 hour, 3 hours, 6 hours, and 24 hours. For each period, we will calculate the annual maximum (e.g., the maximum 3-hour accumulation of each year), then apply the same algorithm in W2013. Not all the stations can be used for every period. For the 15-minute accumulation period, we can only use the site data at CLM (Table 5.1) and the

15-minute NWS data (Table 5.2). For the 1 hour periods, we can use the CLM 15-minute datasets aggregated to 1 hour, plus hourly NWS data (Table 5.2). Those same datasets are also aggregated to create the 3- and 6-hour datasets. For the 24-hour accumulation period, we can use all the collected data – CLM data aggregated to 24 hours, hourly NWS data aggregated to 24 hours, and daily data from the eleven site gauges (Table 5.1).

W2013 applies a correction to this data to account for the fact that a rainfall event may begin during one recording period and end during another, possibly forcing a strong event to be recorded as two weaker ones. This will have a stronger effect on shorter accumulation intervals, and W2013 corrected for this with multiplication factors (originally from W98) to be applied to each interval (Table 5.3). For the 15-minute interval (CLM and NWS data), the recorded data are multiplied by 1.13, while the data both recorded hourly (NWS data) and 15 minute CLM data aggregated to hourly are multiplied by the same factor when the one-hour interval is studied (Table 5.3). When these hourly and 15-minute data are both aggregated to create three- and six-hour datasets, smaller factors are applied. For the 24-hour interval, the sub-daily recorded data are recorded by the small factor of 1.01, while the data recorded daily are multiplied by 1.13.

Table 5.3 Multiplication factors for Annual Maximum, as per W98.

Accumulation Interval	Multiplication Factor
15 minutes	1.13
1 hour	1.13
3 Hours	1.03
6 Hours	1.02
24 Hours	1.01/1.13

5.2 Extreme Value Theory

Section 5.4 of DOE-STD-1020-2016 calls for probabilistic modeling of future precipitation totals. As with the wind data, we will take the time series of annual precipitation maxima at all stations, use them to create a non-exceedance pdf by fitting the same distributions (Eqs. 8), then read the desired extreme values from the tail. The major difference is that we must repeat this for various accumulation periods. We first select an accumulation period, then aggregate (if required) the data at each station to match (e.g., calculate all one-hour accumulations from the 15-minute data (Fig. 5.1)). Then, we select the maximum value within each year, normalize the time series as in Eq. 7, and apply the same procedure to obtain the non-exceedance probability (Eqs. 8).

a)

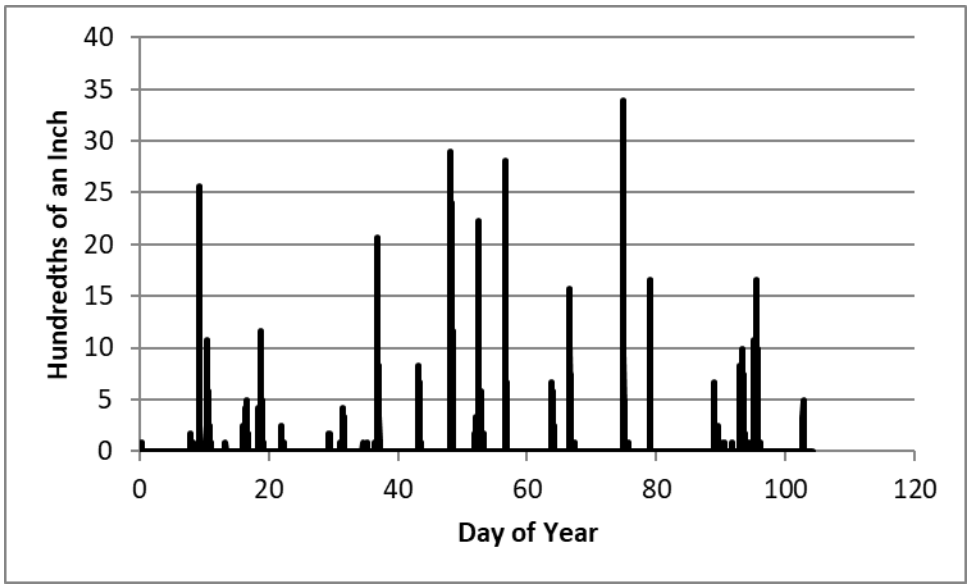

b)

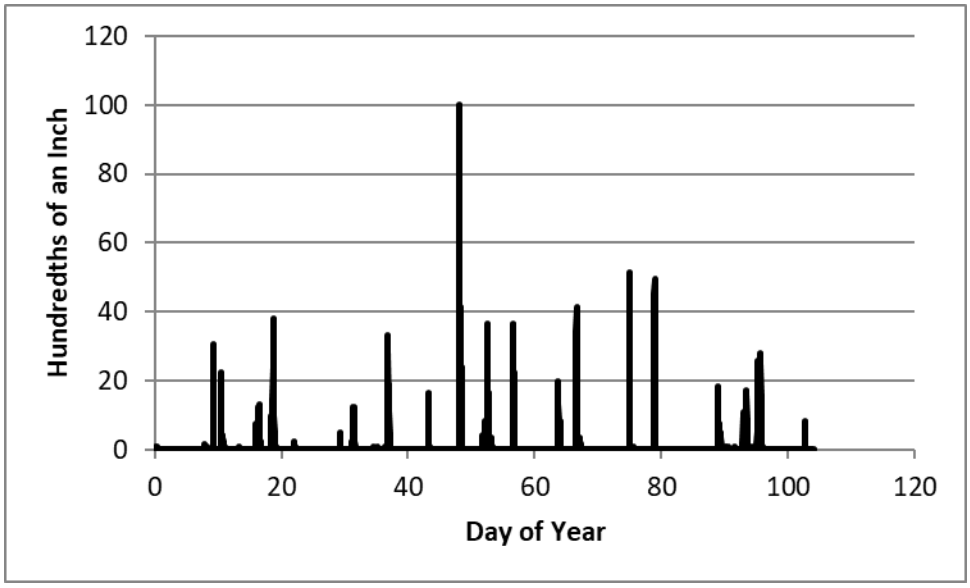

Figure 5.1 a) Time series of annual maximum 15-minute precipitation readings for the CLM for 2008. b) The same series, now aggregated to 1 hour accumulation periods.

5.3 Results for Precipitation

As in Section 4.2, we will calculate the terms in Eqs. 15 (by solving for κ and Z) and correlate the LHS and RHS of each to estimate the degree to which each distribution best fits the data.

Table 5.4 shows the correlation values, and one thing stands out - for all averaging periods, the correlations are very close, making it difficult to conclude that one is superior to the other. Therefore, we apply both the Z statistic and the values for the return periods to decide which distribution to use:

1. For 15 minutes, the Z value is very large (and $\kappa > 0$), suggesting GEV3 should be used. However, this distribution produces a curve that bends to the right, producing lower values than the GEV1 distribution. Given the small correlation difference and the desire to maintain a conservative estimate, we will use a GEV1 distribution to forecast the future precipitation probabilities.
2. For 1 hour, we will use GEV1 – the Z value is within the -1.96 to 1.96 range and GEV1 also has higher values.
3. For 3 hours, the correlation values are similar, and Z is low, so it too will use GEV1.
4. For 6 and 24 hours, the magnitudes of Z are larger (though still within the +/- 1.96 range). With values of $\kappa < 0$, however, the GEV2 distributions have higher values, so we elect to use that distribution for these accumulation periods.

Table 5.4 Correlation values between the LHS and RHS of Eqs. 15.

	κ	Z	Eq. 15a	Eq.15b
15 Minutes	.26	4.35	0.978	0.996
1 Hour	.041	0.83	0.993	0.995
3 Hours	-.037	-0.75	0.988	0.990
6 Hours	-.075	-1.52	0.995	0.997
24 Hours	-.052	-1.98	0.995	0.993

After deciding on a distribution, we can now use Eqs. 18 and 23 to calculate the total precipitation values associated with each return period for the different accumulation periods. (All results are listed in Appendix A). For the 15-minute accumulation period, we are limited to only four datasets (Table 5.5), with annual maximum averages that vary from ~0.77”-0.85”. The projected accumulation totals (Fig. 5.2) vary from between 1-1.5” for a 10-year period, to about 2.8” for 10^5 years, about 1/4 inch lower than in W2013.

Table 5.5 Data for the annual maxima for 15-Minute accumulated precipitation.

Station	Average Peak Rainfall (inches)	Std. Deviation of Peak Rainfall (inches)
SRS/CLM	.77	.18
Clark Hill	.79	.20
Louisville	.85	.20
Wagener	.85	.29

Figure 5.2 Projected (GEV 1) 15-minute precipitation totals for various return periods at SRS, along with values from the W2013 report.

For a one-hour period, the averages range from about 1.47” to 1.58”. The expected accumulations (Figure 5.3) generally range from about 2.5” for a 10-year period to 7” for 10^5 years (similar to W2013).

Table 5.6 Data for the annual maxima for the 1-hour accumulated precipitation.

Station	Average Peak Rainfall (inches)	Std. Deviation of Peak Rainfall (inches)
SRS/CLM	1.58	0.48
Clark Hill	1.47	0.52
Louisville	1.49	0.54
Wagener	1.55	0.58

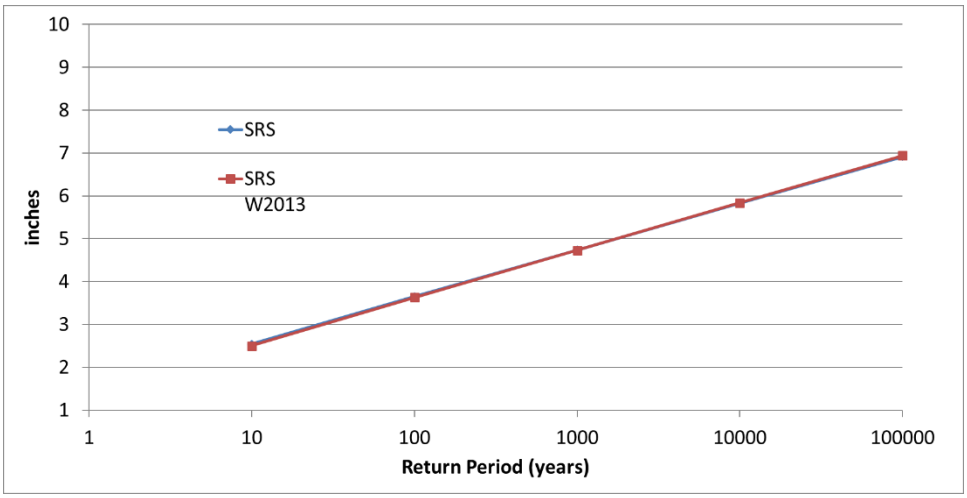

Figure 5.3 Projected (GEV 1) 1-hour accumulation totals for various return periods at SRS, along with values from the W2013 report.

When the data from the same stations used previously are aggregated to three-hour accumulation periods before creating a time series of the annual maximum of each year, the averages range from about 2.1”-2.3” (Table 5.7). SRS can expect to see about 9” every 10^5 years within a single 3-hour period (Figure 5.4).

Table 5.7 Data for the annual maxima for the 3-hour accumulated precipitation.

Station	Average Peak Rainfall (inches)	Std. Deviation of Peak Rainfall (inches)
SRS/CLM	2.25	0.61
Clark Hill	2.08	0.87
Louisville	2.11	0.75
Wagener	2.16	0.82

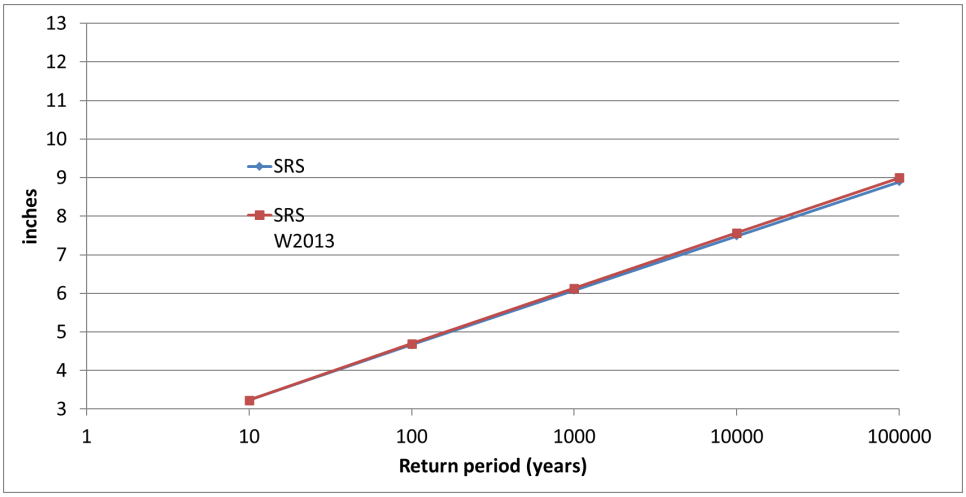

Figure 5.4 Projected 3-hour (GEV1) accumulation totals for various return periods at SRS, along with values from the W2013 report.

Extending the period to six-hours (Table 5.8), averages now range from 2.5”-2.7”.

We can now expect >~10” every 10^5 years (Fig. 5.5). For 24-hour accumulations, we include the SRS gauge data from Table 5.1, and the station averages now range from about 3.1” to 3.5” (Table 5.9). With this data, we can expect values of ~5” every 10 years, with over 15” every 10^5 years (Fig. 5.6).

Table 5.8 Data for the annual maxima for the 6-hour accumulated precipitation.

Station	Average Peak Rainfall (inches)	Std. Deviation of Peak Rainfall (inches)
SRS/CLM	2.69	0.71
Clark Hill	2.50	1.10
Louisville	2.56	0.87
Wagener	2.54	0.93

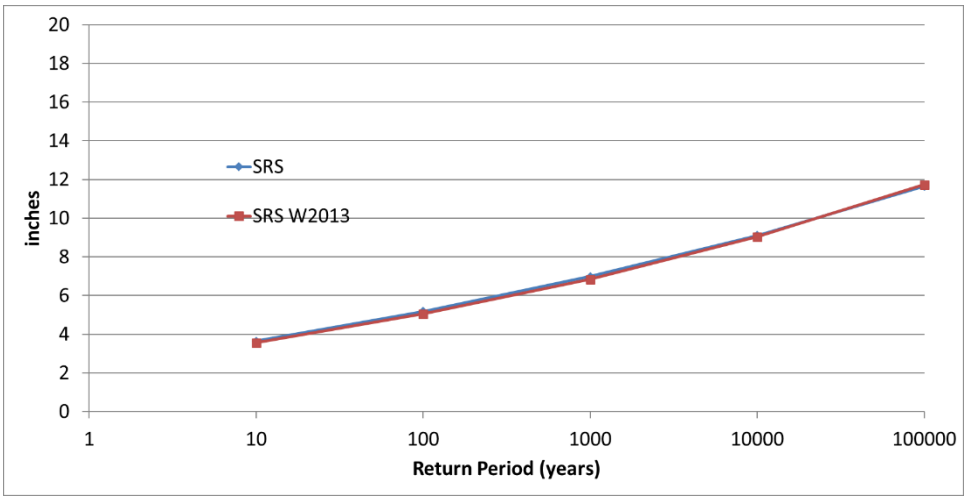

Figure 5.5 Projected (GEV 2) 6-hour accumulation totals for various return periods at SRS, along with values from the W2013 report.

Table 5.9 Data for the annual maxima for the 24-hour accumulated precipitation.

Station	Average Peak Rainfall (inches)	Std. Deviation of Peak Rainfall (inches)
SRS/CLM	3.54	1.01
Clark Hill	3.51	1.43
Louisville	3.47	1.01
Wagener	3.28	1.13
700-A	3.34	1.17
BARR2	3.41	.963
BARR3	3.25	1.00
BARR5	3.32	1.11
100-C	3.15	.98
400-D	3.28	1.07
200-F	3.28	.93
200-H	3.44	.99
100-K	3.48	1.21
100-L	3.48	1.18
100-P	3.26	1.11
SRTC	3.48	1.11

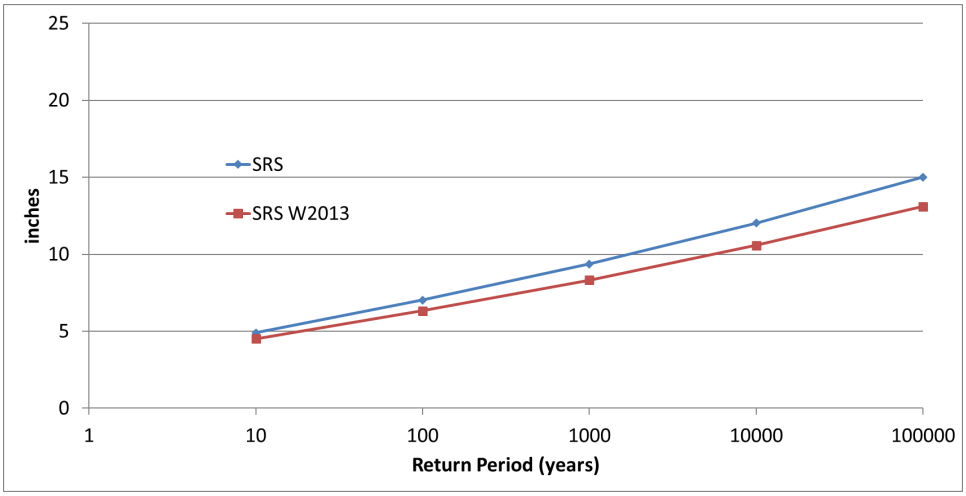

Figure 5.6 Projected (GEV 2) 24-hour accumulation totals for various return periods at SRS, along with values from the W2013 report.

DOE-STD-1020-2016, Section 7.4.1 (their Table 7-1) requires precipitation amounts for four return periods – 500 years, 2000 years, 10,000 years, and 25,000 years – that correspond to the 'Design Basis' for flooding at different 'precipitation design categories' (PDC), and these are listed in Table 5.10 for the different accumulation periods. That same document also requires a 'Structural Loads' design basis (their Table 7-2), with 4 different return periods, and these are listed in Table 5.11. The NRC requires nuclear power plants to be designed based on a flood (design basis flood) produced by the probable maximum precipitation (PMP) storm, which is defined as the greatest rainfall theoretically possible over given duration intervals and river basin drainage areas (USNRC, 2021). Maps of PMP for rainfall durations from 6 hr to 72 hr and drainage areas from 10 km^2 to 20,000 km^2 are given in Schreiner and Riedel (1978). For SRS, the PMP for 6-hr and 24-hr duration events for a drainage area of 518 km^2, closest to the

area of the Upper Three Runs Creek basin, were estimated from the appropriate maps. These values are listed in Table 5.10.

Table 5.10 Peak precipitation values (inches) for DOE-mandated return periods for Design Basis Flooding at SRS/CLM.

Return Period (years)	15 Minutes	1 hour	3 hours	6 hours	24 hours
500 (PDC-1)	1.86	4.41	5.65	6.41	8.64
2000 (PDC-2)	2.11	5.07	6.50	7.58	10.14
10,000 (PDC-3)	2.39	5.83	7.49	9.11	12.02
25,000 (PDC-4)	2.56	6.26	8.05	10.07	13.17
PMP*				22.90	34.50

Table 5.11 Peak precipitation values (inches) for DOE-mandated return periods for Design Basis Structural Loads at SRS/CLM.

Return Period (years)	15 Minutes	1 hour	3 hours	6 hours	24 hours
100 (PDC-1)	1.58	3.65	4.67	5.18	7.02
200 (PDC-2)	1.70	3.98	5.09	5.69	7.70
2500 (PDC-3)	2.15	5.18	6.64	7.78	10.39
6250 (PDC-4)	2.32	5.61	7.20	8.65	11.46

The National Oceanic and Atmospheric Administration (NOAA) calculates frequency precipitation estimates and publishes them as part of its Atlas-14 Frequency Analysis of the United States. Volume 2 of that document has data for South Carolina, and was last updated in 2006. For comparison, we include the 10yr, 100yr and 1000yr values (Table 5-12). At all accumulation periods, the Atlas-14 values were slightly higher at the lower return periods, but about 1-3 inches higher at the 1000-year interval.

Table 5.12 Comparison of peak precipitation values (inches) for DOE-mandated return periods for the Atlas-14 values and the current analysis (W25).

Return Period (years)	15 Minutes		1 hour		3 hours		6 hours		24 hours	
	Atlas	W25	Atlas	W25	Atlas	W25	Atlas	W25	Atlas	W25
10	1.36	1.16	2.57	2.54	3.18	3.22	3.77	3.65	5.29	4.90
100	1.78	1.57	3.76	3.65	4.98	4.67	6.01	5.18	8.39	7.02
1000	2.16	1.98	5.12	4.74	7.39	6.08	9.11	6.99	12.5	9.37

6.0 Quality Assurance

To ensure the accuracy of the reported methods and results, an independent internal review was performed. This review examined written calculations, computer programs and Microsoft Excel® charts for proper equations and consistency between the different formats.

Meteorological data taken from sources located onsite at SRS have previously undergone quality assurance review and are deemed acceptable for use in this report (Weinbeck et al., 2020). Datasets obtained from the NCDC should already have undergone quality control as well for removal of bad data points. Missing data in these datasets was replaced with zeroes and were mainly used to ensure proper processing of the dataset. The primary difficulties in compiling the tornado set are the differences in reporting between datasets and the differences in tornado classification before and after 2007. These were addressed using methods published in peer-reviewed articles.

Methods for calculating the return periods and extreme value theory used for straight-line winds and precipitation are grounded in peer-reviewed literature and regulatory documents from DOE. Analysis of the hand-calculations confirms that these methods are being properly computed. The results are sound and fit within expected ranges based on the available data.

Based on the independent review, it was determined that the reported methodology agreed with the procedures used by the authors. Further, no mistakes were found in the authors' calculations.

In addition to the internal, independent checking and review process by SRNL, an external, independent peer review of the report was performed by Eric Kabela of ORNL. The comments received were all editorial in nature. SRNS requested a follow up question: "are the approaches and methodologies employed by SRNL technically sound and defensible?", and this was confirmed by the reviewer.

References

American National Standard, 2024: *Determining Meteorological Information at Nuclear Facilities*, ANSI/ANS-3.11-2024, American Nuclear Society, La Grange Park, IL

American National Standard, 2011: Estimating Tornado, Hurricane, and Extreme Straight Line Wind Characteristics at Nuclear Facility Sites, ANSI/ANS-2.3-2011, American Nuclear Society, La Grange Park, IL

Boissonnade, A., Q. Hossain, J. Kimball, R. Mensing, and J. Savy, 2000: Development of a Probabilistic Tornado Wind Hazard Model for the Continental United States Volume 1: Main Report, UCRL-ID-140922-VOL-1

Eliasson, J., 1997: A statistical model for extreme precipitation, *Water Resources Research*, **33**, 449-455

Hosking, J., J. Wallis, and E. Wood, 1985: Estimation of the Generalized Extreme-Value Distribution by the Method of Probability-Weighted Moments, *Technometrics*, **27**, 251-261

Lu, D., 1995: A Statistically Rigorous Model for Tornado Hazard Assessment, Master Thesis, Texas Tech University

McDonald, J. R., 1983: A Methodology for Tornado Hazard Probability Assessment, Prepared for Division of Health, Siting and Waste Management Office of Nuclear Regulatory Research, U. S. Nuclear Regulatory Commission, Washington, D.C.

Ramsdell, J., and J. Rishel, 2007: Tornado Climatology of the Contiguous United States, PNNL, NUREG/CR-4461, Rev. 2

Reinhold, T. A., and B. Ellingwood. 1982: Tornado Damage Risk Assessment. NUREG/CR-2944, U.S. Nuclear Regulatory Commission, Washington, D.C.

Schreiner, L., and J. Riedel, 1978: Probable Maximum Precipitation Estimates, United States East of the 105th Meridian, Hydrometeorological Report No. 51, U. S. Department of Commerce, Washington, DC

Scott, K. E., 2013: Savannah River Site Annual Meteorology Report for 2012, SRNL-RP-2013-00070, Savannah River National Laboratory, Aiken SC.

Smith, B., T. Castellanos, A. Winters, C. Mead, A. Dean, R. Thompson, 2013: Measured Severe Convective Wind Climatology and Associated Convective Modes of Thunderstorms in the Contiguous United States, 2003–09. *Wea. Forecasting*, **28**, 229–236.

USDOE, 2011: Radiation Protection of the Public and the Environment, DOE Order 458.1, Washington DC.

USDOE, 2015: *Environmental Radiological Effluent Monitoring and Environmental Surveillance*, DOE-HDBK-1216-2015.

USDOE, 2016: Natural Phenomena Hazards Analysis and Design Criteria for DOE Facilities, DOE-STD-1020-2016, Washington, DC.

USNRC, 2021: Considerations for Estimating Site-Specific Probable Maximum Precipitation at Nuclear Power Plants in the United States of America, Final Report, NUREG/KM-0015, ORNL/SPR-2021/1375,

Weber, A. H., 1998: Tornado, Maximum Wind Gust, and Extreme Rainfall Event Recurrence Frequencies at the Savannah River Site, WSRC-TR-98-00329.

Weber, A., 2002: Wind Climate Analyses for National Weather Service Stations in the Southeast (U), WSRC-TR-2002-00515

Weinbeck S, Viner B, Rivera-Giboyeaux A., 2020: Meteorological Monitoring Program at the Savannah River Site. SRNL-TR-2020-00197, available at https://weather.srs.gov/atg/static/pdf/SRNL-TR-2020-00197.pdf

Werth, D., A. Weber, and G. Shine, 2013: Probabilistic Hazard Assessment for Tornadoes, Straight-line Wind, and Extreme Precipitation at the Savannah River Site, SRNL-STI-2013-00664

WSRC (Washington Savannah River Company), 2004: Savannah River Site DSA Support Document – Site Characteristics and Program Descriptions, WSRC-IM-2004-00008.

Appendix A

Precipitation Extreme Values

	Return Period Values (inches) for Different Accumulation Periods				
Return Period (years)	15 Minutes	1 Hour	3 Hours	6 Hours	24 Hours
10	1.16	2.54	3.23	3.65	4.90
100	1.58	3.65	4.67	5.18	7.02
1000	1.99	4.74	6.08	6.98	9.37
10000	2.40	5.83	7.49	9.11	12.02
100000	2.81	6.92	8.90	11.64	15.01
1000000	3.22	8.00	10.30	14.64	18.36
1.00E+07	3.60	9.01	11.61	17.95	21.87

Distribution:

C. Tuma (NNSA), 730-B

R. Williams (SRS), 730-4B

S. Carey (SRS), 730-4B

S. R. Chiswell, 773-A

B. J. Viner, 773-A